

# Feshbach resonances and their interaction in light scattering off photonic crystal slabs

I. Evenor <sup>a</sup>, E. Grinvald <sup>a,\*</sup>, F. Lenz <sup>b,†</sup> and S. Levit<sup>a,‡</sup>

<sup>a</sup> *Department of Condensed Matter  
The Weizmann Institute of Science  
Rehovot Israel*

<sup>b</sup> *Institute for Theoretical Physics III  
University of Erlangen-Nürnberg  
Staudstrasse 7, 91058 Erlangen, Germany*

(Dated: July 20, 2011)

## Abstract

The concept of Feshbach resonances developed for quantum mechanical scattering is applied in the analysis of classical light scattering off photonic crystal slabs. It is shown that this concept can be realized almost perfectly in these systems. As an application guided-mode resonances in the grating waveguide structure (GWS) are studied in detail. Using simple resonance dominance approximation the characteristic properties of isolated Feshbach resonances in light scattering are exhibited. Formation and interaction of overlapping resonances are investigated. The relevant parameters of the GWS are identified which control the shape of the reflectivity of interacting resonances as well as the enhancement of the electromagnetic field. The differences in the properties of TE and TM resonances is emphasized for both isolated and interacting resonances.

---

\*Electronic address: eran.grinvald@weizmann.ac.il

†Electronic address: flenz@theorie3.physik.uni-erlangen.de

‡Electronic address: shimon.levit@weizmann.ac.il

## I. INTRODUCTION

A general property of scattering of waves, e.g., of light or matter waves is the appearance of resonances. Resonances are observed in acoustic waves as well as in scattering of waves associated with elementary particles at wavelengths ranging from meters to  $10^{-15}$  m. Crudely speaking there are two classes of resonances, the shape (or potential) resonances and Feshbach resonances. Shape resonances occur in a variety of classical and quantum mechanical systems in which wavelength and the size of the resonator or target are of the same order of magnitude.

The concept of Feshbach resonances [1, 2] on the other hand applies to quantum mechanical scattering on many-body systems such as atomic nuclei [3] and has found recently important applications in atomic and molecular physics [4, 5]. A Feshbach resonance occurs if the kinetic energy of the incident particle is close to an almost stable intermediate “molecular” state. In the field of cold atoms, it has been instrumental that the condition for appearance of Feshbach resonances can be manipulated by tuning the strength of an external magnetic field to which the magnetic moments of the atoms are coupled.

In this work we will show that Feshbach resonances occur in the very different context of scattering of light off photonic crystal slabs. The fundamental mechanism for the formation of resonances is the process of turning a bound state (guided mode) into a resonance “state” (barely radiating mode).

We will focus our studies on a particular photonic crystal slab - the grating waveguide structure (GWS). Guided mode resonances in GWS have been studied both theoretically and experimentally since 1985, Refs. [6, 7], and have already been incorporated into a wide variety of applications, cf. Refs. [8–13]. Theoretically they have been investigated using several different approaches including a scattering matrix approach [14], temporal coupled mode theory [15, 16], Wigner-Weisskopf formalism [17] as well as coupled mode theory [18]. In the majority of these theoretical approaches parameter fitting is required to make comparison with exact numerical calculations [19, 20]. Our approach is similar to the coupled mode approach of Rosenblatt et al. [18] which was in turn based on the work of Kazarinov et al. in distributed feedback lasers [21]. Yet the origin of our treatment is different being based on the formalism of Feshbach resonances. In this way are able to derive accurate analytical expressions for essentially all resonance properties. Miroshnichenko [22, 23] and others [24] have pointed out that various photonic resonances can be treated as Fano-Feshbach resonances, yet since no analytic expressions for the coupling exist a parameter fitting procedure had to be used. In addition most of the theories concentrated on the properties of the TE resonances. To the best of our knowledge none of the fully analytic theories of guided mode resonances treated the TM polarized resonances and their differences from the TE resonances.

As in the case of atomic physics, the light scattering off GWS will be shown to be tunable in a variety of ways generating isolated as well as overlapping Feshbach resonances. We will apply a simple resonance dominance approximation and will obtain essentially analytic expressions for all relevant observables. In this way we will provide the tools to produce resonances with properties desired in applications by adjusting the GWS parameters. The resonance dominance approximation will also allow us to study systematically the interaction of two or more Feshbach resonances.

## II. RESONANCE SCATTERING OF LIGHT - FORMAL DEVELOPMENT

In this section we will develop a formalism which will make explicit the role of Feshbach resonances in light scattering off photonic crystals. For this purpose and as an example we will consider the so called grating waveguide structure [18] (GWS) which consists of a plane waveguide with one dimensional grating on the top of it. The left part of Fig. 1 shows an example of a GWS with piecewise constant grating layer where the waveguide, the grating, the substrate and the superstrate layers are shown as well as the incident, reflected and transmitted light. The right part of the figure shows the corresponding dielectric function where we replaced the grating layer  $\epsilon_{II}(x)$  with a homogeneous layer with an effective dielectric constant  $\epsilon_0$ . The exact definition of  $\epsilon_0$  depends on the polarization of the incident light, cf. Eq. (6) and Eq. (33) below. In our formal studies we will treat on equal footing both piecewise constant as well as continuous transitions of  $\epsilon$  between the dielectric layers.

In the present work we investigate only the case of classical incidence where the incident light wave vector is perpendicular to the grating grooves, i.e.  $k_y = 0$ . We start with the TE polarization. The modifications needed for the TM case will be considered in Section II B.

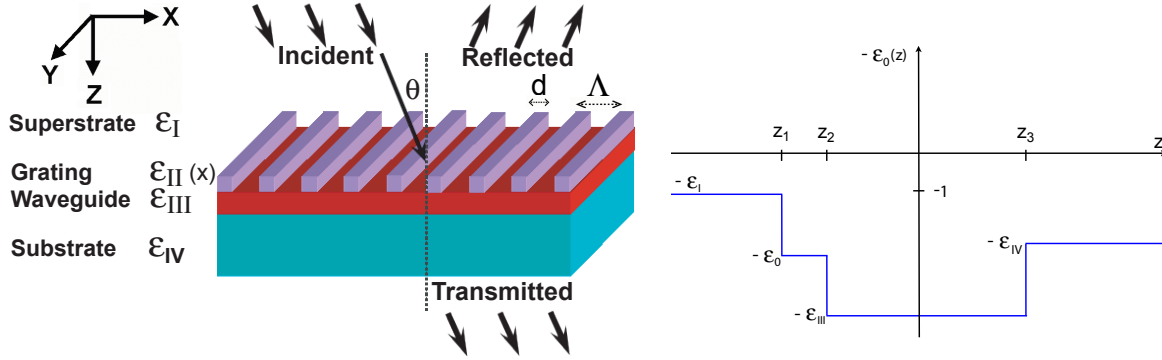


FIG. 1: Left: Light incident on a grating waveguide structure (GWS) composed of piecewise  $z$ -independent layers with dielectric constants  $\epsilon_I \dots \epsilon_{IV}$ . The geometry of the grating layer (II) is characterized by the grating period  $\Lambda$  and the duty cycle  $d/\Lambda$ . Right: Polarization dependent effective dielectric constant (cf. Eqs. (6) and (33)) as a function of  $z$  for the GWS on the left.

### A. TE waves

In the TE polarization the electric field of the incident light is parallel to the grating grooves which in our geometry (cf. Fig. 1) implies

$$\mathbf{E}(\mathbf{r}) = E(x, z) \mathbf{e}_y. \quad (1)$$

The stationary Maxwell equation for a time harmonic electric field of frequency  $\omega$  (with the speed of light set to unity)

$$\nabla \times \nabla \times \mathbf{E}(\mathbf{r}) = \epsilon(\mathbf{r}) \omega^2 \mathbf{E}(\mathbf{r}), \quad (2)$$

then simplifies to

$$\left( -\frac{\partial^2}{\partial z^2} - \frac{\partial^2}{\partial x^2} - \epsilon(x, z) \omega^2 \right) E(x, z) = 0. \quad (3)$$

To describe light incident on GWS from  $z \rightarrow -\infty$  with the wave vector in the  $x$ - $z$  plane  $\mathbf{k} = (k_x, 0, k_z)$  we impose the boundary conditions that for  $z \rightarrow \infty$  we have only an outgoing wave. With this choice the asymptotic behavior of  $E(x, z)$  is

$$\lim_{z \rightarrow -\infty} E(x, z) = e^{ik_x x} (e^{ik_z^- z} + r(\omega, k_x) e^{-ik_z^- z}) , \quad \lim_{z \rightarrow \infty} E(x, z) = t(\omega, k_x) e^{ik_x x} e^{ik_z^+ z} . \quad (4)$$

The choice of the normalization is free and, as is common, we have normalized the amplitude of the incident wave to be 1. As a consequence, the reflected and transmitted fields are given in units of the incident field. The quantities  $r(\omega, k_x)$  and  $t(\omega, k_x)$  are respectively the reflection and transmission amplitudes. One of our goals is to devise a simple method to calculate these amplitudes and to show that their resonant behavior is typical of Feshbach resonances. Note that  $k_x^2 + (k_z^-)^2 = \epsilon_I \omega^2$  while  $k_x^2 + (k_z^+)^2 = \epsilon_{IV} \omega^2$

The  $x$ -dependence of the dielectric constant is limited to the grating layer ( $z_1 < z < z_2$ ). It is periodic with the grating period  $\Lambda$

$$\epsilon(x + \Lambda, z) = \epsilon(x, z) . \quad (5)$$

and can be represented in terms of its Fourier-components

$$\epsilon_n(z) = \frac{1}{\Lambda} \int_{-\Lambda/2}^{\Lambda/2} dx \epsilon(x, z) e^{-inK_g x} . \quad (6)$$

Here we consider real valued  $\epsilon(x, z)$

$$\epsilon_{-n}(z) = \epsilon_n^*(z) . \quad (7)$$

If  $\epsilon(x, z)$  is symmetric or antisymmetric around an appropriately chosen center of the elementary interval, the Fourier-components  $\epsilon_n(z)$  are real or imaginary respectively. In the coordinate system shown in Fig.1, the periodicity of  $\epsilon(x, z)$  implies that the  $x$  dependence of  $E(x, z)$  contains only Fourier components with the discrete  $x$ -components of the wave vectors of the form

$$k_x + nK_g , \quad K_g = \frac{2\pi}{\Lambda} . \quad (8)$$

Inserting

$$E(x, z) = \sum_{n=-\infty}^{\infty} E_n(z) e^{-i(k_x + nK_g)x} , \quad (9)$$

into Eq. (3) we rewrite the latter as a system of ordinary differential equations (here and in the following we will suppress the summation limits  $\pm\infty$ )

$$\left( -\frac{d^2}{dz^2} + (k_x + nK_g)^2 - \epsilon_0(z)\omega^2 \right) E_n(z) = \omega^2 \sum_{m \neq n} \epsilon_{n-m}(z) E_m(z) . \quad (10)$$

To see what the asymptotic conditions (4) imply for this system we note that for  $m \neq n$   $\epsilon_{n-m}(z) = 0$  when  $z \rightarrow \pm\infty$  so that the equations decouple at large  $|z|$ . We will further assume that we deal with the so called subwavelength zero order grating, i.e. such that

$$\omega^2 - (k_x + nK_g)^2 \geq 0 \quad \text{only for } n = 0 .$$

Therefore all the components  $E_n(z)$  with  $n \neq 0$  are required to decay exponentially with  $z \rightarrow \pm\infty$ . The non vanishing asymptotic conditions (4) apply only to  $E_0(z)$

$$\lim_{z \rightarrow -\infty} E_0(z) = e^{ik_z^- z} + r(\omega, k_x) e^{-ik_z^- z} \quad , \quad \lim_{z \rightarrow \infty} E_0(z) = t(\omega, k_x) e^{ik_z^+ z} . \quad (11)$$

We convert (10) into a system of integral equations and introduce to this end the Green's functions satisfying

$$\left( -\frac{d^2}{dz^2} + (k_x + nK_g)^2 - \epsilon_0(z)\omega^2 \right) g_n(z, z') = -\delta(z - z') , \quad (12)$$

and obtain

$$E_n(z) = E_0^{(+)}(z)\delta_{n0} - \omega^2 \int dz' g_n(z, z') \sum_{m \neq n} \epsilon_{n-m}(z') E_m(z') . \quad (13)$$

Here we use the fact that light is incident only in the  $n = 0$  channel. The term  $E_0^{(+)}(z)\delta_{n0}$  satisfies (10) with vanishing right hand side so that  $E_0^{(+)}(z)$  is a solution of

$$\left( -\frac{d^2}{dz^2} + k_x^2 - \epsilon_0(z)\omega^2 \right) E_0^{(+)}(z) = 0 . \quad (14)$$

and we impose the same boundary condition as in Eq. (4) with reflection and transmission amplitudes which we will denote by  $r_0(\omega, k_x)$  and  $t_0(\omega, k_x)$  respectively. It is the  $z$ -dependent part of the electric field  $E_0^{(+)}(z)e^{ik_x x}$  which propagates in and is scattered off the effective dielectric structure defined by  $\epsilon_0(z)$  shown in the right part of Fig. 1. We will refer to this scattering as “background scattering” upon which Feshbach resonances are formed by coupling to guided modes. In Appendix VI B the appropriate “background” Green's function is explicitly constructed.

Systems of equations of coupled channels such as Eqs. (10, 13) are underlying the description of Feshbach resonances in atomic and nuclear physics. A Feshbach resonance occurs if, by neglecting certain couplings, a bound state of the entire system exists. Accounting for the couplings converts this state into a resonance. In this spirit let us consider the above system (10) in absence of the coupling  $\epsilon_n(z) = 0$ ,  $n \neq 0$  of the Fourier components  $E_n(z)$ . In this approximation, the photonic crystal slab is described by the effective dielectric constant in the right part of Fig. 1 and the resulting guided modes are the progenitors of Feshbach resonances.

As the wave functions of bound states in quantum mechanics, guided modes in dielectric slabs are localized in the  $z$ -direction

$$z \rightarrow \pm\infty , \quad E(x, z) \rightarrow 0 , \quad (15)$$

and are determined by the eigenvalue equation

$$\left( -\frac{d^2}{dz^2} - \epsilon_0(z)\omega^2 \right) \mathcal{E}_\eta(z) = \eta \mathcal{E}_\eta(z) , \quad (16)$$

with the frequency dependent eigenvalues  $\eta = \eta(\omega)$ . The electric field is given by

$$E(x, z) = e^{i\beta x} \mathcal{E}_\eta(z) . \quad (17)$$

Inserting this ansatz into the wave equation (cf. Eq. (3))

$$\left(-\frac{\partial^2}{\partial z^2} - \frac{\partial^2}{\partial x^2} - \epsilon_0(z)\omega^2\right)E(x, z) = 0, \quad (18)$$

the dispersion relation between frequency  $\omega$  and the x-component  $\beta$  of the wave vector is obtained

$$\beta^2 = -\eta(\omega). \quad (19)$$

In Fig. (2) we show as an example the dispersion curves of the first three TE and TM guided modes for a medium with the z-dependent dielectric constant  $\epsilon_0(z)$  of Fig. (1) and numerical values of the dielectric constant given in Eqs. (57) and (58)

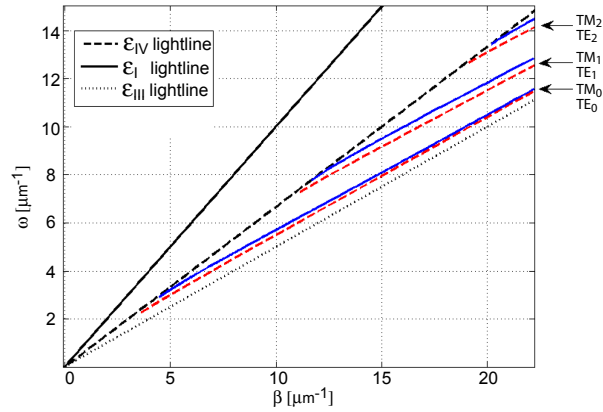


FIG. 2: Guided mode frequencies  $\omega_i(\beta)$  as a function of the propagation constant  $\beta$  for a medium with the z-dependent dielectric constant  $\epsilon_0(z)$  of Fig. (1). The numerical values of the dielectric constants are given in Eqs. (57) and (58) and  $i$  is the mode order. Dashed curves are for TE guided modes (red color online), solid curves TM (blue color online). Also shown are the lightlines  $\omega = \beta/\sqrt{\epsilon}$  for  $\epsilon_I$ ,  $\epsilon_{III}$  and  $\epsilon_{IV}$ .

The subset of equations (13) with  $n \neq 0$  can be rewritten as

$$E_n(z) = - \int dz' \left\{ \sum_i \frac{\mathcal{E}_{\eta_i}(z)\mathcal{E}_{\eta_i}(z')}{-\eta_i - (k_x + nK_g)^2} + G_c(z, z') \right\} \omega^2 \sum_{m \neq n} \epsilon_{n-m}(z') E_m(z'), \quad (20)$$

where the first term in the curly brackets is the contribution of the guided modes  $\mathcal{E}_{\eta_i}(z)$  to the the Green's function  $g_n(z, z')$  (cf. Eq. (12)) and  $G_c(z, z')$  the contribution of the continuum (radiating) modes. The guided modes are described by normalizable functions and we require

$$\int_{-\infty}^{\infty} dz \mathcal{E}_{\eta_i}(z) \mathcal{E}_{\eta_i}^*(z) = 1. \quad (21)$$

With this exact reformulation of the original wave equation we are in the position to formulate the criterion for appearance and dominance of Feshbach resonances. Theoretically, an isolated Feshbach resonance is expected to occur for sufficiently small coupling ( $\epsilon_n(z)$   $n \neq 0$ ) and if the kinematics ( $k_x$  and  $\omega$ ) is chosen such that (cf. Eq. (20))

$$\eta_i + (k_x + nK_g)^2 \approx 0. \quad (22)$$

In this case the scattering of light will be dominated by one of the terms in the discrete part of the spectrum, i.e., by one of the guided modes localized in  $z$ . The coupling to the extended mode delocalizes these modes and turns them thereby into resonances, i.e., guided modes become “slightly radiating”. Narrow subwavelength resonances in this system were observed (cf. Refs. [11, 18, 25–27]) in a wide range of the parameters, i.e. wavelength, angle of incidence and the dielectric structure parameters. This supports the assumption of weak coupling of the guided to the extended modes.

The criterion (22) is essentially identical to the quantum mechanical criterion for Feshbach resonances which requires that the incident energy coincides approximately with that of a “molecular” state which in the limit of vanishing coupling becomes a true bound state. As in scattering of ultracold atoms, the properties of the Feshbach resonances can be manipulated in light scattering as well. They can be tailored towards a particular application by variation of the parameters of the system or externally by using electro-optical materials[28].

For the analysis of the resonances observed in scattering of light off photonic crystal slabs the reformulation of the wave equation (3) by the system of equations ((12), (20)) suggests to neglect for  $n \neq 0$  the continuum contributions to the Greens functions  $g_n(z, z')$ , i.e., to approximate Eq. (20) by

$$E_n(z) \approx \omega^2 \int dz' \sum_i \frac{\mathcal{E}_{\eta_i}(z) \mathcal{E}_{\eta_i}(z')}{\eta_i + (k_x + nK_g)^2} \sum_{m \neq n} \epsilon_{n-m}(z') E_m(z'), \quad n \neq 0. \quad (23)$$

We will refer to this approximation as “resonance dominance”. In general the condition (22) is satisfied for one guided mode only and the contributions from the other guided modes can be neglected. With a judicious choice of the parameters, a simultaneous excitation of two or more Feshbach resonances can be achieved and the interaction of these “overlapping” resonances can be studied. A particular class of two interacting Feshbach resonances will be discussed later.

Notwithstanding the formal connection between Feshbach resonances in quantum mechanical scattering of particles and in classical scattering of TE polarized light the content of the corresponding wave equations is very different. We mention in particular the role of the frequency. The Maxwell equation (2) implies that the frequency plays a twofold role. On the one hand, both in quantum mechanics and in electrodynamics, the frequency determines the asymptotic properties of the incident particle or light. Simultaneously in electrodynamics, the frequency also determines the strength of the interaction of light with the dielectric medium. Peculiar consequences are the frequency dependence of the eigenvalues  $\eta$  and the electric fields of the guided modes  $\mathcal{E}_\eta(z)$  (cf. Eq.(16)) as well as the independence of these quantities on the x-component of the wave vector. As we will see below, these properties not only distinguishes TE modes from quantum mechanical waves but also from the TM modes.

## B. TM waves

In many aspects the treatment of the TM polarization is identical to the TE case so we will present it briefly. In the TM polarized waves the magnetic field is parallel to the grating grooves which in our geometry means that

$$\mathbf{H}(\mathbf{r}) = H(x, z) \mathbf{e}_y. \quad (24)$$

Inserting this into the Maxwell equation (we set  $c=1$ )

$$\nabla \times \frac{1}{\epsilon(\mathbf{r})} \nabla \times \mathbf{H} = \omega^2 \mathbf{H} \quad (25)$$

we obtain

$$\left[ -\partial_x \frac{1}{\epsilon(x, z)} \partial_x - \partial_z \frac{1}{\epsilon(x, z)} \partial_z \right] H(x, z) = \omega^2 H(x, z). \quad (26)$$

As discussed in [29] this equation is analogous to a Schrodinger equation in two dimensions with no potential but coordinate dependent mass. Accordingly we write it in the form

$$\Theta H = \omega^2 H \quad (27)$$

where

$$\Theta = -\partial_x \frac{1}{\epsilon(x, z)} \partial_x - \partial_z \frac{1}{\epsilon(x, z)} \partial_z. \quad (28)$$

As in the TE case we need to solve the above equation under the condition that only outgoing wave is present at  $z \rightarrow \infty$

$$\lim_{z \rightarrow -\infty} H(x, z) = e^{ik_x x} (e^{ik_z^- z} + r(\omega, k_x) e^{-ik_z^- z}) \quad , \quad \lim_{z \rightarrow \infty} H(x, z) = t(\omega, k_x) e^{ik_x x} e^{ik_z^+ z} \quad (29)$$

where as before  $r(\omega, k_x)$  and  $t(\omega, k_x)$  are respectively the reflection and transmission amplitudes for the present TM scattering. Using the analog of the expansion in Eq. (9)

$$H(x, z) = \sum_{n=-\infty}^{\infty} H_n(z) e^{-i(k_x + nK_g)x}, \quad (30)$$

and inserting in (27) we obtain a set of coupled equations similar to (10)

$$[\omega^2 - \Theta_{nn}] H_n(z) = \sum_{m \neq n} \Theta_{nm} H_m(z), \quad (31)$$

where we introduced

$$\Theta_{nm} = -\partial_z \gamma_{n-m}(z) \partial_z + (k_x + nK_g)(k_x + mK_g) \gamma_{n-m}(z), \quad (32)$$

and defined

$$\gamma_n(z) \equiv \frac{1}{\Lambda} \int_{-\Lambda/2}^{\Lambda/2} dx \frac{1}{\epsilon(x, z)} e^{-inK_g x}. \quad (33)$$

The effective dielectric constant  $\epsilon_0(z)$  shown in Fig.1 is (for the TM polarization) just  $1/\gamma_0(z)$ .

We note that there exist an ambiguity in our definition of  $\gamma_{n-m}(z)$  in (32). If we view it as a matrix  $\gamma_{nm}(z)$  we can either use the above definition  $\gamma_{nm}(z) = \gamma_{n-m}(z)$  as given by Eq. (33) or we could also have defined it as the inverse of the matrix  $\epsilon_{n-m}$  with  $\epsilon_n$  given by Eq. (6). We will comment upon and test this ambiguity below in our numerical examples.

As in the TE case the subwavelength grating condition imply that all the components  $H_n(z)$  with  $n \neq 0$  should have exponential decay as the boundary conditions at  $z \rightarrow \pm\infty$ . The zeroth component  $H_0(z)$  should asymptotically behave as

$$\lim_{z \rightarrow -\infty} H_0(z) = e^{ik_z^- z} + r(\omega, k_x) e^{-ik_z^- z} \quad , \quad \lim_{z \rightarrow \infty} H_0(z) = t(\omega, k_x) e^{ik_z^+ z}. \quad (34)$$



Let us now convert the set (31) into integral equations similar to what we did in Eq. (13)

$$H_n(z) = H_0^{(+)}(z)\delta_{n0} + \int dz' g_n(z, z') \sum_{m \neq n} \Theta_{nm} H_m(z'), \quad (35)$$

where in analogy to Eq. (14) the component  $H_0^{(+)}(z)$  and the Green's functions  $g_n(z, z')$  solve respectively the differential equations

$$[\omega^2 - \Theta_{00}]H_0^{(+)}(z) = 0, \quad (36)$$

and

$$[\omega^2 - \Theta_{nn}]g_n(z, z') = \delta(z - z'). \quad (37)$$

Here  $H_0^{(+)}(z)$  describes the TM scattering off the effective structure defined by  $\epsilon(z) = \gamma_0^{-1}(z)$ . As in the TE case we choose it to satisfy the boundary conditions similar to (34) denoting the corresponding reflection and transmission amplitudes by  $r_0(\omega, k_x)$  and  $t_0(\omega, k_x)$  respectively. Accordingly we chose the boundary conditions for the Green's function  $g_0(z, z')$  such that the full solution  $H_0(z)$  satisfies Eq. (34).

It is useful to consider the eigenfunctions of the operators  $\Theta_{nn}$  with different  $n$ 's

$$\Theta_{nn}\mathcal{H}_{n,\nu}(z) = \eta_{n,\nu}\mathcal{H}_{n,\nu}(z). \quad (38)$$

Note that for each  $n$  there is a complete set of eigenfunctions  $\mathcal{H}_{n,\nu}(z)$  with the corresponding eigenvalues  $\eta_{n,\nu}$  distinguished by the index  $\nu$ .

From the comparison with the Maxwell equation (26) one can easily see that the eigenfunctions  $\mathcal{H}_{n,\nu}(z)$  determine the  $z$  dependent part of the TM photonic modes with propagation constant  $k_x + nK_g$  and frequency  $\omega_{n,\nu}^2 = \eta_{n,\nu}$ ,

$$H_{(k_x+nK_g),\nu}(x, z) = e^{i(k_x+nK_g)x}\mathcal{H}_{n,\nu}(z) \quad (39)$$

of the effective structure defined by  $\epsilon(z) = \gamma_0^{-1}(z)$ . We will call such a structure "unperturbed". We will base the treatment of the effects of the  $x$ -dependence of the grating upon solutions for this structure which we assume known.

We now concentrate on the equations (35) with  $n \neq 0$  and use the spectral representation of  $g_n(z, z')$  as in Eq. (20)

$$H_n(z) = \int_{I_g} dz' \left\{ \sum_i \frac{\mathcal{H}_{n,\nu_i}(z)\mathcal{H}_{n,\nu_i}(z')}{\omega^2 - \eta_{n,\nu_i}} + G_c(z, z') \right\} \sum_{m \neq n} \Theta_{nm} H_m(z') \quad (40)$$

where the first term in the curly brackets is the contribution of the guided modes (denoted by discrete index  $\nu_i$ ) to the the Green's function  $g_n(z, z')$  while  $G_c(z, z')$  is the contribution of the continuum.

We have assumed the normalization of the guided modes

$$\int_{-\infty}^{\infty} dz \mathcal{H}_{n,\nu_i}(z) \mathcal{H}_{n,\nu_i}^*(z) = 1. \quad (41)$$

Note that since  $\Theta_{nm}$  with  $n \neq m$  is vanishing outside the grating interval  $I_g$ , the integrals in (40) are over  $I_g$

As in the TE case our main approximation will consist in neglecting the continuum contributions to the Greens functions  $g_n(z, z')$  for  $n \neq 0$ . Thus we approximate Eq. (40) as

$$H_n(z) = \int_{I_g} dz' \left\{ \sum_i \frac{\mathcal{H}_{n,\nu_i}(z) \mathcal{H}_{n,\nu_i}(z')}{\omega^2 - \eta_{n,\nu_i}} \right\} \sum_{m \neq n} \Theta_{nm} H_m(z'). \quad (42)$$

This is the “resonance dominance” approximation in the TM case. An isolated TM Feshbach resonance occurs when the physical parameters are such that

$$\eta_{n,\nu_i} \approx \omega^2 \quad (43)$$

and the contributions from the other guided modes can be neglected. Of special interest to us will also be cases of a simultaneous excitation and interaction of two or more Feshbach resonances.

### III. ISOLATED RESONANCES

#### A. TE resonances

In this section we will discuss in detail properties of an isolated Feshbach resonance. By comparison with the results of exact numerical evaluations, we will determine the degree of validity of resonance dominance in light scattering. To be concrete, we will carry out this study in the grating waveguide structure (GWS) as shown on the left in Fig. 1. The grating, periodic in  $x$  (cf. Eq. (5)), is restricted in the  $z$ -direction to the region II which we denote as the grating interval  $I_g$ . The effective dielectric constant is given by (cf. Eq. (6) and the right part of Fig. 1)

$$\epsilon_0(z) = \epsilon_I \theta(z_1 - z) + \epsilon_0 \theta(z - z_1) \theta(z_2 - z) + \epsilon_{III} \theta(z - z_2) \theta(z_3 - z) + \epsilon_{IV} \theta(z - z_3). \quad (44)$$

while

$$\epsilon_n(z) = \epsilon_n \theta(z - z_1) \theta(z_2 - z) \quad \text{for } n \neq 0. \quad (45)$$

In these expressions  $\epsilon_n$  denote constants given by Eq. (6) for the layered structure when  $z$  is restricted to the grating interval.

Let us assume that these parameters of the GWS as well as the angle of illumination and the frequency are such that the condition (22) is satisfied for a single value of  $n = \nu$  and a particular eigenvalue  $\eta_0$  of the guided mode equation (16). Let us denote by  $\mathcal{E}_{\eta_0}$  the corresponding eigenfunction. Beyond the resonance dominance (cf. Eq. (23)) we truncate the system of equations ((13), (23)) further and take into account only two modes, the extended mode of the incident light ( $n=0$ ) and the guided mode ( $\eta_0$ ,  $n = \nu$ ). We thus reduce the system of equations (13) to

$$E_0(z) = E_0^{(+)}(z) - \epsilon_{-\nu} \omega^2 \int_{I_g} dz' g_0(z, z') E_\nu(z'), \quad (46)$$

$$E_\nu(z) = \frac{\epsilon_\nu \omega^2}{\eta_0 + (k_x + \nu K_g)^2} \mathcal{E}_{\eta_0}(z) \int_{I_g} dz' \mathcal{E}_{\eta_0}(z') E_0(z'), \quad (47)$$

and for simplicity will refer to this combined approximation to “resonance dominance”. This system can be solved analytically. As Eq. (47) shows the resonance component of the electric field  $E_\nu$  is proportional to the resonating guided mode

$$E_\nu(z) = \sigma_\nu \mathcal{E}_{\eta_0}(z) \quad (48)$$

with the proportionality coefficient  $\sigma_\nu$  measuring the degree of the excitation of the guided mode. Inserting this expression for  $E_\nu(z)$  into Eq. (46), multiplying the resulting equation with  $\mathcal{E}_{\eta_0}(z)$  and integrating we obtain the following expression for the field enhancement coefficient

$$\sigma_\nu = \epsilon_\nu \omega^2 \frac{\mathcal{C}^{(+)}}{\rho}, \quad (49)$$

with  $\mathcal{C}^{(\pm)}$  denoting the coupling to the guided mode  $\mathcal{E}_{\eta_0}$  of the electric fields  $E_0^{(\pm)}(z)$  incident from either  $-\infty$  or  $\infty$  (cf. Eq. (153) for their precise definitions),

$$\mathcal{C}^{(\pm)} = \int_{I_g} dz \mathcal{E}_{\eta_0}(z) E_0^{(\pm)}(z). \quad (50)$$

The integral is carried out over the grating interval  $I_g$ . The denominator in (49)

$$\rho = \eta_0 + (k_x + \nu K_g)^2 + |\epsilon_\nu|^2 \omega^4 \Sigma, \quad (51)$$

contains the resonance condition (cf. Eq. (22)) modified by the “self-coupling”  $\Sigma$  of the guided mode

$$\Sigma = \int_{I_g} dz \int_{I_g} dz' \mathcal{E}_{\eta_0}(z) g_0(z, z') \mathcal{E}_{\eta_0}(z'). \quad (52)$$

$\Sigma$  is generated by transitions from the guided to the extended mode, the propagation in the extended mode and then the back transition to the guided mode. The strength of this contribution to  $\rho$  is determined by the corresponding Fourier coefficient  $\epsilon_\nu$  of the dielectric function (cf. Eqs. (6), (7), (45)).  $\Sigma$  is complex with the imaginary part accounting for the loss of intensity from the guided to the extended mode. It gives rise to a shift of the resonance position and to a width. Using the identity (160) derived in Appendix B, the following expression for the width of the resonance is obtained

$$\frac{\tilde{\Gamma}}{2} = -|\epsilon_\nu|^2 \omega^4 \text{Im} \Sigma = \frac{\omega^4}{2k_z^-} |\epsilon_\nu \mathcal{C}^{(+)}|^2, \quad (53)$$

with the z-component of the wave vectors  $k_z^\pm$  defined in Eq. (152). The strength  $\sigma_\nu$  of the guided mode excitation also determines the resonance behavior of reflection and transmission amplitudes which are found from asymptotics of  $E_0(z)$  in Eq. (46). Using the expression for  $g_0(z, z')$  and its asymptotics derived in the Appendix B (Eq. (157)) as well Eq. (48) we find

$$r(\omega, k_x) - r_0(\omega, k_x) = \frac{i}{2k_z^-} \sigma_\nu \epsilon_{-\nu} \omega^2 \mathcal{C}^{(+)} = -\frac{i}{2k_z^- - \eta_0 - (k_x + \nu K_g)^2 - |\epsilon_\nu|^2 \omega^4 \Sigma} |\epsilon_\nu|^2 \omega^4 \mathcal{C}^{(+)^2}. \quad (54)$$

Similarly the corresponding expression for the transmission amplitude is obtained (cf. Eq. (151))

$$t(\omega, k_x) - t_0(\omega, k_x) = \frac{i}{2k_z^+} \sigma_\nu \epsilon_{-\nu} \omega^2 \mathcal{C}^{(-)} = -\frac{i}{2k_z^+ - \eta_0 - (k_x + \nu K_g)^2 - |\epsilon_\nu|^2 \omega^4 \Sigma} |\epsilon_\nu|^2 \omega^4 \mathcal{C}^{(+)} \mathcal{C}^{(-)}. \quad (55)$$

Reflection and transmission amplitudes are related to each other. The resonance dominance approximation shares with the exact system of equations the property of power conservation. It is straightforward to derive the following identity

$$|r(\omega, k_x)|^2 + \frac{k_z^+}{k_z^-} |t(\omega, k_x)|^2 = 1, \quad (56)$$

which is valid irrespective of the number of guided modes. It thus applies to the case of isolated as well as overlapping resonances which we study below and is easily generalized to the case when more than one extended mode is present.

The background scattering is not only present in the first term in Eq. (46) and in the reflection and transmission amplitudes  $(r_0, t_0)$ . It also affects the resonance terms via  $\mathcal{C}^{(+)}$  and  $\Sigma_\nu$ , Eqs. (50) and (52). Only in this way it is possible to have the absolute squares of the total reflection and transmission amplitudes  $r(\omega, k_x)$ ,  $t(\omega, k_x)$  satisfying the identity (56) (cf. also Eq. (152)). The interference between background and resonance contributions will be one source of the asymmetry of the shape of the resonance curve akin to the phenomenon of Fano resonances in quantum mechanical systems [30, 31].

Fan et al. [16] have previously shown that the reflectivity curves for guided mode resonance can be described analytically as Fano resonances where the spectral bandwidth of the resonance is an external fitting parameter from exact numerical simulations. Our investigations support their claim and in addition produce the full analytic form of the resonant width (cf. Eqs. 49-55), including the weak spectral dependence of  $\Sigma$ .

In general, the background scattering also exhibits resonances. These shape resonances owe their existence to the properties of the “potential”  $\omega^2 \epsilon_0(z)$  (Eq. (44)) and do not involve transformation of a localized mode into a (delocalized) resonance.

We have restricted our numerical studies to GWS with piecewise constant dielectric structures. Minor changes only are required to account for a general  $z$ -dependence. We have to replace

$$\epsilon_\nu \mathcal{C}^{(\pm)} \rightarrow \int dz \mathcal{E}_{\eta_0}(z) \epsilon_\nu(z) E_0^{(\pm)}(z), \quad |\epsilon_\nu|^2 \Sigma \rightarrow \int dz \int dz' \mathcal{E}_{\eta_0}(z) \epsilon_\nu(z) g_0(z, z') \epsilon_{-\nu}(z) \mathcal{E}_{\eta_0}(z').$$

In all our numerical studies we kept fixed the thickness of the layers and the dielectric constant of the superstrate. Using the notation of Eqs. (44) and (45)

$$\ell_g = z_2 - z_1 = 0.1 \mu m, \quad \ell = z_3 - z_2 = 0.4 \mu m, \quad \epsilon_I = 1. \quad (57)$$

In the first application we choose the following profile of the grating interval, the dielectric constants, the grating period  $\Lambda$ , the duty cycle  $d/\Lambda$  and the grating contrast  $\epsilon_g - 1$

$$\begin{aligned} \epsilon_{II}(x) &= \left[ 1 + (\epsilon_g - 1) \theta(d^2 - x^2) \right] \theta(x - x_0) \theta(\Lambda + x_0 - x), \\ \epsilon_{III} &= 4, \quad \epsilon_{IV} = 2.25, \quad \Lambda = 0.81 \mu m, \quad d = \frac{\Lambda}{2}, \quad \epsilon_g = 4. \end{aligned} \quad (58)$$

These parameters have been chosen such that, for the wavelength  $\lambda = 1.5 \mu m$  and the angle  $\theta = 5^\circ$  of the incident light, the extended mode resonates with the guided mode with  $\nu = -1$  (cf. Eqs. (46), (47)).

The numerical evaluation of the expression for the reflection amplitude (54) proceeds in two steps. In the first step, the extended  $E_0^\pm(z)$  and guided  $\mathcal{E}_{\eta_0}(z)$  modes together with the

guided mode eigenvalue  $\eta_0$  are calculated for the effective medium (44) where the dielectric constant in the grating layer is replaced by its averaged value  $\epsilon_0 = 2.5$  for the choice of the grating profile (58) and the parameters (58). The functions  $E^\pm(z)$  and  $\mathcal{E}_{\eta_0}$  have an analytic form and only the eigenvalue  $\eta_0$  requires numerical solution of a transcendental equation. Given these building blocks it is straightforward to calculate in the second step observables such as the reflectivity, the electric field, etc..

The eigenvalue  $\eta_0$  as a function of  $\omega^2$  and the electric fields of the guided modes are displayed in Fig. 3. The numerical results of the evaluation of Eq. (54) are presented on the

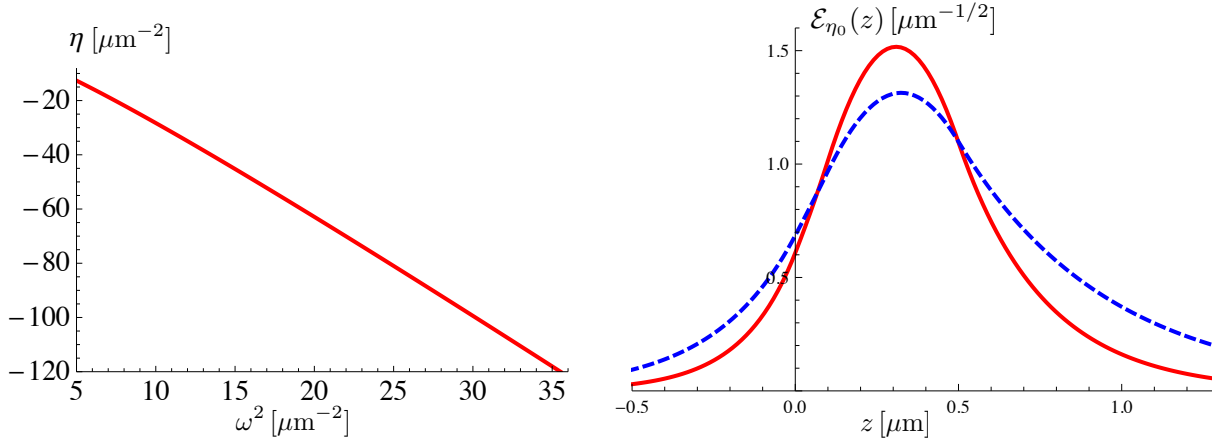


FIG. 3: Results for GWS with parameters specified in Eqs.(57)-(58). Left: the eigenvalue  $\eta$  (cf. Eq. (16)) as a function of  $\omega^2$ . Right: normalized electric fields of guided modes for  $\lambda = 1.5 \mu\text{m}$  (solid) and  $2.1 \mu\text{m}$  (dashed line).

left of Fig. 4.

In order to assess the accuracy of our theory we have compared it with numerical results obtained by applying transfer matrix techniques (cf. [32]) to the system of equations (10) truncated to a finite number of channels. Convergence was typically achieved with 5-10 channels. We shall refer to these converged results as "exact". Such exact values of the resonance position  $\lambda_{\text{res}}$  and the full width at half maximum  $\Gamma$  are

$$\lambda_{\text{res}} = 1.5000 \mu\text{m}, \quad \Gamma = 3.91168 \text{ nm}. \quad (59)$$

The deviations from these values obtained when truncating the coupled equations (10) to just two (i.e.  $n = -1$  and  $n = 0$ ) and in the resonance approximation are respectively

$$\delta\lambda_{\text{res}} = -0.6 \text{ nm}, \quad \delta\Gamma = -0.0087 \text{ nm}, \quad \delta\lambda_{\text{res}} = -0.6 \text{ nm}, \quad \delta\Gamma = -0.0129 \text{ nm}. \quad (60)$$

The exact resonance position is shifted by  $\delta\lambda_{\text{res}} = 17.4 \text{ nm}$  relative to the eigenvalue of the guided mode. The resonance dominance approximation reproduces this shift as well as the resonance width with an accuracy of 3.3 %.

The coupling of the  $\nu = -1$  guided mode to other guided modes neglected in this simplest version of the resonance dominance approximation is the most likely mechanism to account for the few % deviation of the resonance position from the exact result. It is not difficult to show that, independent of any details, the resulting shift due to such additional couplings is always towards longer wavelengths. In addition, the essentially identical results obtained in

resonance dominance and at the lowest level truncation rule out a significant contribution from the  $\nu = -1$  continuum contributions (cf. Eq. (20)).

Similar results and the same level of agreement have been found for other values of the angle of the incident light. In order to enhance the effect of the background scattering and to study in detail the changing shapes generated by the interference between resonance and background contributions (Fano resonances) we have changed to the following parameters of the dielectric medium (cf. Eq. (58)),

$$\epsilon_{IV} = 1, \quad \Lambda = 1 \mu m. \quad (61)$$

With this choice one finds a strong background reflection with  $|r_0(\omega, , k_x)| = 0.9$ . As shown in the right part of Fig.4, as a result, a drastic change in the shape of the resonance curve is obtained due the interference between background and resonance amplitudes. To facilitate the comparison we have shifted the resonance dominance curve by 0.75 nm. An almost perfect agreement is observed indicating that the interference between background and resonance amplitudes is treated correctly.

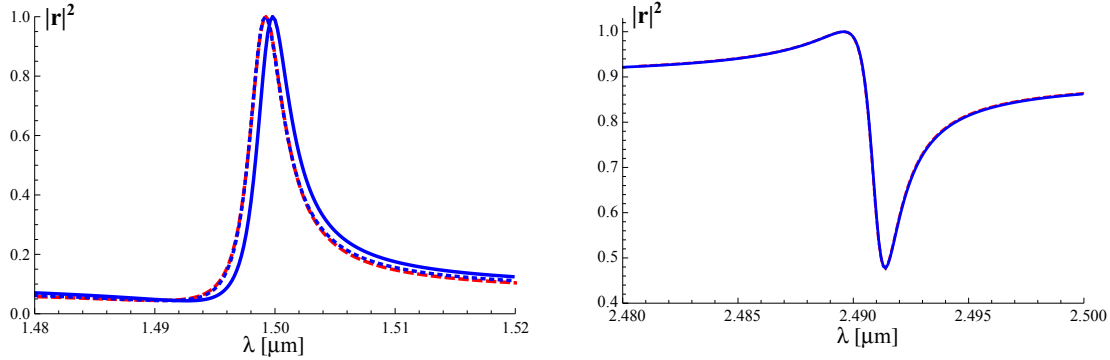


FIG. 4: Reflectivity (cf Eq. (54)) as a function of the wavelength. Left: angle of incidence  $5^\circ$  and parameters of the GWS specified in Eqs.(57)-(58). Solid lines: exact values, dashed lines: values obtained in the resonance dominance approximation. Dotted line (in the left figure and coinciding with the dashed line): values obtained by truncation of Eq. (20) to  $n, m = 0, -1$ , see the text. Right: angle of incidence  $75^\circ$  with changes in the parameters (cf. Eq. (61)). Solid line: exact values, dashed lines: values obtained in the resonance dominance approximation and shifted by 0.75 nm towards larger wavelengths to facilitate the comparison.

A peculiar feature of the TE case in sharp contrast to quantum mechanical scattering is the dependence of the strength of the interaction of light with the dielectric on the frequency  $\sim (\epsilon(x, z) - 1)\omega^2$  (cf. Eq. (3)). This implies that the eigenvalues and eigenfunctions of the guided mode equation (16) depend on the frequency (cf. Fig.3). At the same time, as in quantum mechanics, the frequency determines asymptotically the behavior of the incident or scattered light. As a consequence of this twofold role of the frequency, the observables like width and position of the resonance have a rather intricate dependence on the frequency. To illustrate the consequences we consider the width and expand the resonance denominator  $\rho$  (51) around  $\omega_r$ , the zero of its real part

$$\text{Re } \rho(\omega_r) = 0, \quad \rho(\omega) \approx \gamma(\omega - \omega_r - i\gamma^{-1}|\epsilon_\nu|^2\omega_r^4 \text{Im } \Sigma(\omega_r)), \quad (62)$$

with

$$\gamma = (K_g - \omega_r \sin \theta) \sin \theta + \left[ 2\omega \frac{d\eta_0}{d\omega^2} - |\epsilon_\nu|^2 \frac{d}{d\omega}(\omega^4 \text{Re } \Sigma) \right]_{\omega=\omega_r}. \quad (63)$$

In the range of frequencies of interest to us, the dominant contribution to  $\gamma$  arises from the second term. Without a frequency dependent interaction,  $\gamma \approx -2\omega_r$ . Instead, as can be read off from Fig. 3, we find  $\gamma \approx -7\omega_r$ . Thus the frequency dependence of the interaction leads to a significant narrowing of the resonance structure.

## B. TM resonances

We consider here the simplest case when only one resonating term, i.e. a term with small denominator is present in the sums over the modes in Eq. (40). We stress that our assumption means that such a term occurs only for one particular value of  $n$ , i.e. that the resonant condition (43) is fulfilled for one particular pair  $(n, \nu_i)$ . We denote it by  $(k, \kappa)$ . We approximate by truncating the system (35) to only two equations - that of  $n = 0$  (in which the incoming light appears) and the resonating  $n = k$ . This is the truncation approximation. It leads to two coupled equations

$$H_0(z) = H_0^{(+)}(z) + \int_{I_g} dz' g_0(z, z') \Theta_{0k} H_k(z'), \quad (64)$$

$$H_k(z) = \int_{I_g} dz' \left\{ \sum_{\nu} \frac{\mathcal{H}_{k,\nu}(z) \mathcal{H}_{k,\nu}(z')}{\omega^2 - \eta_{k,\nu}} \right\} \Theta_{k0} H_0(z'). \quad (65)$$

Furthermore in the equation for  $H_k$  we retain only the resonating mode  $k, \kappa$ . This is the approximation of the resonance dominance. We thus obtain

$$H_0(z) = H_0^{(+)}(z) + \int_{I_g} dz' g_0(z, z') \Theta_{0k} H_k(z'), \quad (66)$$

$$H_k(z) = \frac{\mathcal{H}_{k,\kappa}(z)}{\omega^2 - \eta_{k,\kappa}} \int_{I_g} dz' \mathcal{H}_{k,\kappa}(z') \Theta_{k0} H_0(z'). \quad (67)$$

Exactly as in the TE case this system of equations can be solved analytically, cf., Eqs. (46,47). Equation (67) shows that the  $H_k(z)$  is just proportional to the guiding mode  $\mathcal{H}_{k,\kappa}(z)$

$$H_k(z) = \sigma \mathcal{H}_{k,\kappa}(z) \quad , \quad \sigma = \frac{1}{\omega^2 - \eta_{k,\kappa}} \int_{I_g} dz' \mathcal{H}_{k,\kappa}(z') \Theta_{k0} H_0(z'). \quad (68)$$

Inserting  $H_k(z) = \sigma \mathcal{H}_{k,\kappa}(z)$  in (66) we obtain

$$H_0(z) = H_0^{(+)}(z) + \sigma \int_{I_g} dz' g_0(z, z') \Theta_{0k} \mathcal{H}_{k,\kappa}(z'). \quad (69)$$

We then multiply both sides of this equality by  $\mathcal{H}_{k,\kappa}(z) \Theta_{k0}$ , integrate over  $z$  and solve for the field enhancement coefficient  $\sigma$ . We obtain

$$\sigma = \frac{\mathcal{C}^{(+)}}{\omega^2 - \eta_{k,\kappa} - \Sigma}, \quad (70)$$

where we have introduced

$$\mathcal{C}^{(\pm)} = \int_{I_g} dz \mathcal{H}_{k,\kappa}(z) \Theta_{k0} H_0^{(\pm)}(z), \quad (71)$$

$$\Sigma = \int_{I_g} dz dz' \mathcal{H}_{k,\kappa}(z) \Theta_{k0} g_0(z, z') \Theta_{0k} \mathcal{H}_{k,\kappa}(z'). \quad (72)$$

Here  $H_0^{(-)}$  is the matching pair of the solution  $H_0^{(+)}$  as defined in the TM part of Appendix VI B.

Equations (68) through (72) provide a complete solution of the problem. It is expressed through the solutions  $H_0^{(+)}(z)$  and  $\mathcal{H}_{k,\kappa}$  of the unperturbed structure. From (69) one can easily extract the reflection and transmission amplitudes from the asymptotic behavior of  $H_0(z)$  and  $g_0(z, z')$ . Using Appendix VI B we obtain

$$\begin{aligned} \lim_{z \rightarrow -\infty} H_0(z) &= e^{ik_z^- z} + r e^{-ik_z^- z}, \quad r = r_0 - \frac{i\epsilon_I}{2k_z^-} \frac{|\gamma_k|^2 \tilde{\mathcal{C}}^{(+)^2}}{\omega^2 - \eta_{k,\kappa} - \Sigma}, \\ \lim_{z \rightarrow \infty} H_0(z) &= t e^{ik_z^+ z}, \quad t = t_0 - \frac{i\epsilon_{IV}}{2k_z^+} \frac{|\gamma_k|^2 \tilde{\mathcal{C}}^{(+)} \tilde{\mathcal{C}}^{(-)}}{\omega^2 - \eta_{k,\kappa} - \Sigma}. \end{aligned} \quad (73)$$

Here  $r_0$  and  $t_0$  are the "background" values which appear in  $H_0^{(+)}(z)$ . Note also that we have used the replacement  $\Theta_{nm} \rightarrow \gamma_{n-m} \tilde{\Theta}_{nm}$  explained in Appendix VI C where

$$\tilde{\Theta}_{nm} = \overleftarrow{\partial}_z \overrightarrow{\partial}_z + (k_x + nK_g)(k_x + mK_g). \quad (74)$$

to define  $\mathcal{C}^{(\pm)} = \gamma_k \tilde{\mathcal{C}}^{(\pm)}$  with

$$\tilde{\mathcal{C}}^{(\pm)} = \int_{I_g} dz \left[ \partial_z \mathcal{H}_{k,\kappa}(z) \partial_z H_0^{(\pm)}(z) + (k_x + kK_g) k_x \mathcal{H}_{k,\kappa}(z) H_0^{(\pm)}(z) \right], \quad (75)$$

As in the TE case the self coupling  $\Sigma$  which appears in the denominator of (70) and (73) plays a crucial role. Its real part shifts the resonance frequency away from the eigenvalue  $\eta_{k\kappa}$  of the resonating guided mode while the resonance width is given by the imaginary part of  $\Sigma$ .

Although formally the expressions for  $r$  and  $t$  are very similar to those for the TE case one should note the important and crucial differences in the expressions (71,72) for  $\mathcal{C}^{(\pm)}$  and  $\Sigma$  which contain the coupling operators  $\Theta_{mn}$ .

As already mentioned the TM formalism has an ambiguity of using  $\gamma_{m-n}(z)$  as given by Eq. (33). We could alternatively regard  $\epsilon_{m-n}(z)$  as a matrix  $\epsilon_{mn} \equiv \epsilon_{m-n}(z)$  and inverting it to find  $\gamma_{m-n} = (\epsilon^{-1})_{mn}$ . We have found that the second alternative leads to improved comparison with exact results and adopted it in our examples below. We do not have a good argument to justify this improvement. In the literature, cf., Refs [33–37], this ambiguity in the truncation has been discussed and resolved in favor of the "inverse" method by considering the asymptotic convergence properties of the Fourier components of  $H$  (cf. Eq. (30)) which is an important issue in high precision numerical studies.

In our examples below we have used the same parameters of the structure (57) and (58) as in the TE case. In the first step, the extended  $H_0^{\pm}(z)$  and guided  $\mathcal{H}_{k,\kappa}(z)$  modes together with the guided mode eigenvalue  $\eta_{k,\kappa}$  were calculated for the effective medium (44). They were computed analytically apart from finding eigenvalue  $\eta_{k,\kappa}$  which required solving numerically a transcendental equation.

The main difference at this step as compared with the TE case is the peculiar boundary conditions for the derivatives of the solutions at the boundaries. The combinations  $\epsilon_0(z) \partial_z H_0^{\pm}(z)$  and  $\epsilon_0(z) \partial_z \mathcal{H}_{k,\kappa}(z)$  rather than the derivatives themselves must be continuous. This leads to a subtlety when the integrals (71) and (72) for  $\Sigma$  and  $\mathcal{C}^{(\pm)}$  are computed. Since the derivative terms in the operators  $\Theta_{k0}$  and  $\Theta_{0k}$  contain  $\partial_z \epsilon_k(z) \partial_z$  rather than  $\partial_z \epsilon_0(z) \partial_z$



combinations they produce  $\delta$ -function like singularities when acting on  $H_0^\pm(z)$ ,  $\mathcal{H}_{k,\kappa}$  and  $g_0(z, z')$ . We refer to Appendix VIC in which we explain how we dealt with such singularities. Adopting this approach, the quantities  $\Sigma$  and  $\mathcal{C}^{(\pm)}$  essentially can be evaluated analytically with the results used to calculate reflectivity and other observables.

The numerical results for the reflectivity  $|r|^2$  (cf. Eq. (73)) are presented in Fig. 5.

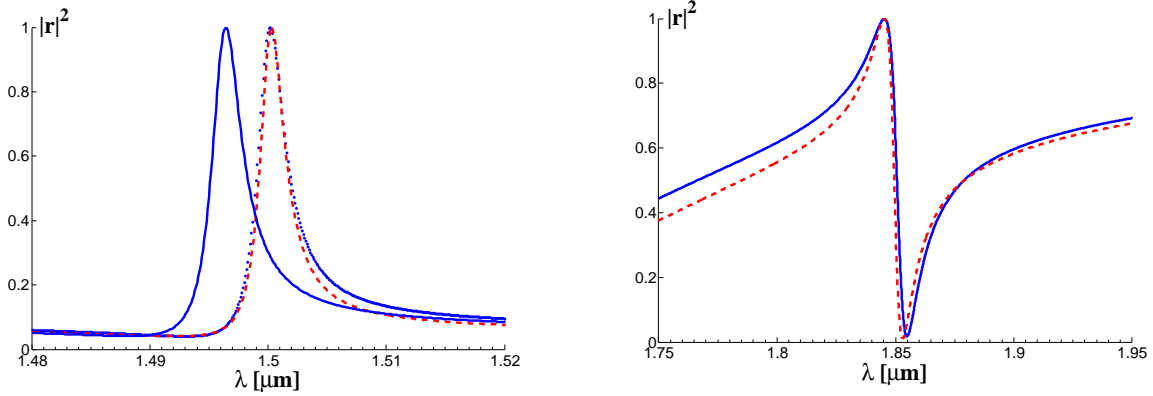


FIG. 5: Reflectivity  $|r(\omega, k_x)|^2$ , cf. Eq. (73), as a function of the wavelength. Left: angle of incidence  $5^\circ$ . The other parameters are as in Eqs. (57)-(58) apart of the grating period which is  $0.87 \mu m$ . Solid lines: exact values, dashed lines: values obtained in the resonance dominance approximation. Dotted line (in the left figure and coinciding with the dashed line): values obtained by truncation of Eq. (31) to  $n, m = 0, -1$ , see the main text. Right: angle of incidence  $86^\circ$  with changes in the parameters to  $\epsilon_{IV} = 1$  and  $\Lambda = 0.8 \mu m$ . Solid line: exact values, dashed lines: values obtained in the resonance dominance approximation and shifted by  $6.4 \text{ nm}$  respectively towards smaller wavelengths.

With the indicated parameters of the grating the resonating guided mode  $\mathcal{H}_{k,\kappa}$  has  $k = -1$  and  $\kappa = 0$ . Our results are compared with numerical results obtained by applying transfer matrix techniques after truncating the system of equations (31). This is similar to what is used in the rigorous coupled wave analysis (RCWA), cf. Ref. [19]. Convergence was typically achieved with 20-30 channels - slower than in the TE case. In the left part of Fig. 5 we also compare with the results of truncation of the system of Eqs. (31) to just two channels,  $n, m = 0, -1$ .

As in the TE case we have also examined the structure parameters for which the Fano interference between the resonance and the background is particularly pronounced. This is shown in the right part of Fig. 5. We observe a good qualitative agreement in both graphs. The same quality of agreement has been found for other values of the angle of the incident light.

At the same time it is seen that on the quantitative level the comparison with the exact results for TM modes is less satisfactory than for the TE modes. For example in the particular resonances of Fig. 5 the discrepancy in the resonance position is  $-3.9 \text{ nm}$  (left) and  $-6.4 \text{ nm}$  (right) as compared to  $0.6 \text{ nm}$  and  $0.7 \text{ nm}$  in the TE case. The discrepancy in the width in the left figure is  $0.639 \text{ nm}$  between the exact results and resonance dominance as compared to just  $-0.013 \text{ nm}$  in the TE case. What is particularly notable is the discrepancy with the two channel truncated results where an almost perfect agreement for the TE case has been obtained.

We tend to attribute these discrepancies to the peculiar TM boundary condition at the borders of the grating layer. These conditions for the guided mode channel are violated in the resonance dominance approximation which we use. We have verified that the discrepancies decrease with decreasing contrast of the grating or decreasing size of the grating interval.

We have also noticed that resonance dominance begins to fail in the TM case for regular binary gratings with very small or very large duty cycle for which  $|\gamma_3| \sim |\gamma_2| \sim |\gamma_1|$ .

A more systematic analysis is required to clarify the above issues. In this respect let us note the following. The general framework for the resonance dominance approximation is provided by the Feshbach projection operators formalism as it is outlined in Appendix VI A. There the exact resonating state is one of the eigenstates in the Q subspace. In our approach we have approximated this state by neglecting the coupling between the Fourier components  $H_n$  with  $n \neq k$ , c.f., Eq. (64). Using an expansion of the modes in terms of Bloch waves rather than plane waves appears as a promising tool to improve the treatment of the TM modes.

## IV. INTERACTION OF FESHBACH RESONANCES

### A. Overlapping TE resonances

#### 1. Formal development

In this section we will extend our discussion and address the issue of overlapping resonances and their interaction. For photonic crystal slabs of the structure shown in Fig. 1 overlapping resonances always exist at illumination close to normal incidence. This has its origin in the time reversal symmetry. It is straightforward to verify that with  $E_n(k_x, k_z^\pm, z)$  also  $E_{-n}^*(-k_x, -k_z^\pm, z)$  solves the system of equations (10) and satisfies the boundary condition (11). This implies that resonances occurring for incident light with  $k_x \rightarrow 0$  always involve two guided modes, i.e. a resonance with  $n = \nu$  is always accompanied by the resonance for  $n = -\nu$ . In the resonance dominance approximation this conclusion follows readily from the resonance condition (22). If it is satisfied for a guided mode  $\mathcal{E}_{\eta_0}(z)$  and  $n = \nu$  at  $k_x \rightarrow 0$  it will also be satisfied for the same guided mode and  $n = -\nu$ . The physics of this condition is that the incoming light with  $k_x \rightarrow 0$  is coupled by the grating to both right ( $\beta = k_x + \nu K_g$ ) and left ( $\beta = k_x - \nu K_g$ ) propagating guided modes having the same  $z$ -profile  $\mathcal{E}_{\eta_0}(z)$ .

We consider in detail this class of overlapping resonances, i.e. we include together with  $E_\nu$  also  $E_{-\nu}$  resulting in a system of equations with 3 components (cf. Eqs. (46), (47))

$$E_0(z) = E_0^{(+)}(z) - \omega^2 \int_{I_g} dz' g_0(z, z') (\epsilon_{-\nu} E_\nu(z') + \epsilon_\nu E_{-\nu}(z')), \quad (76)$$

$$E_{\pm\nu}(z) = \frac{\omega^2}{\eta_0 + (k_x \pm \nu K_g)^2} \mathcal{E}_{\eta_0}(z) \int_{I_g} dz' \mathcal{E}_{\eta_0}(z') (\epsilon_{\pm\nu} E_0(z') + \epsilon_{\pm 2\nu} E_{\mp\nu}(z')). \quad (77)$$

Here we have made use of the peculiar property of the TE modes that the value of  $\nu$  gives rise to shifts of the the eigenvalue  $\eta_0$ ) but does not affect the eigenmode  $\mathcal{E}_{\eta_0}$  (cf. Eq. (16)). According to Eq. (77) the resonance waves  $E_{\pm\nu}(z)$  differ only in their (resonance enhanced) strengths  $\sigma_{\pm\nu}$  (cf. Eq. (48)). Up to these unknown normalizations they are given by the

guided mode  $\mathcal{E}_{\eta_0}$

$$E_{\pm\nu}(z) = \sigma_{\pm\nu} \mathcal{E}_{\eta_0}(z). \quad (78)$$

As in the case of an isolated resonance (cf. Eq. (79)), the reflection amplitude is determined by the asymptotics of  $E_0(z)$  in (76). Using Eqs. (13) and (78) it is easily seen that Eq. (76) is obtained from Eq. (46) by replacing  $\sigma_\nu \epsilon_{-\nu}$  by  $\sigma_\nu \epsilon_{-\nu} + \sigma_{-\nu} \epsilon_\nu$ . Accordingly the expression (54) for the reflection amplitude of an isolated resonance is replaced by

$$r(\omega, k_x) = r_0(\omega, k_x) + \frac{i}{2k_z^-} (\sigma_\nu \epsilon_{-\nu} + \sigma_{-\nu} \epsilon_\nu) \omega^2 \mathcal{C}^{(+)} . \quad (79)$$

It remains to determine the unknown strength parameters  $\sigma_{\pm\nu}$ . To this end one inserts Eq. (76) into the two equations (77) and obtains after using (78) a  $2 \times 2$  linear system system of equations for the unknown variables  $\sigma_{\pm\nu}$ ,

$$W \begin{pmatrix} \sigma_{+\nu} \\ \sigma_{-\nu} \end{pmatrix} = \omega^2 \mathcal{C}^{(+)} \begin{pmatrix} \epsilon_\nu \\ \epsilon_{-\nu} \end{pmatrix} , \quad (80)$$

with the coupling matrix  $W$

$$W = \begin{pmatrix} \eta_0 + (k_x + \nu K_g)^2 + |\epsilon_\nu|^2 \omega^4 \Sigma & \epsilon_\nu^2 \omega^4 \Sigma - \epsilon_{2\nu} \omega^2 V \\ \epsilon_{-\nu}^2 \omega^4 \Sigma - \epsilon_{-2\nu} \omega^2 V & \eta_0 + (k_x - \nu K_g)^2 + |\epsilon_\nu|^2 \omega^4 \Sigma \end{pmatrix} . \quad (81)$$

The diagonal elements of the matrix  $W$  contain the complex valued self interaction  $\Sigma$  defined in Eq. (52). The off-diagonal elements contain a direct coupling via  $\epsilon_{\pm 2\nu}$  between the guided modes with

$$V = \int_{I_g} dz \mathcal{E}_{\eta_0}(z) \mathcal{E}_{\eta_0}(z) , \quad (82)$$

as well as the indirect coupling terms  $\epsilon_\nu^2 \Sigma$  and  $\epsilon_{-\nu}^2 \Sigma$  via the extended mode. In terms of the matrix elements  $W_{ij}$ , the inverse of  $W$  is given by

$$W^{-1} = \frac{1}{W_+ W_-} \begin{pmatrix} W_{22} & -W_{12} \\ -W_{21} & W_{11} \end{pmatrix} , \quad (83)$$

where the eigenvalues of  $W$  are given by

$$W_{\pm} = \eta_0 + k_x^2 + \nu^2 K_g^2 + |\epsilon_\nu|^2 \omega^4 \Sigma \pm \sqrt{(2k_x \nu K_g)^2 + \omega^4 \left( (|\epsilon_\nu|^2 \omega^2 \Sigma - |\epsilon_{2\nu}| \cos \varphi_\epsilon V)^2 + |\epsilon_{2\nu}|^2 \sin^2 \varphi_\epsilon V^2 \right)} . \quad (84)$$

We have introduced the relative phase between  $\epsilon_{2\nu}$  and  $\epsilon_\nu^2$

$$e^{i\varphi_\epsilon} = \frac{\epsilon_{2\nu} \epsilon_\nu^{*2}}{|\epsilon_{2\nu} \epsilon_\nu^2|} , \quad (85)$$

which will be seen to distinguish different types of interacting resonances. The importance of the relative phase between the different Fourier coefficients has been previously emphasized by Barnes et al. [38] in the similar phenomenon of surface plasmon resonance off metallic gratings. Here it is not the relative phase ( $\sim \epsilon_2/\epsilon_1$ ) which matters. Rather the phase  $\varphi_\epsilon$  results from the interference of the 2-step process via the extended mode and the one step

process connecting directly the 2 guided modes. The combination of the strengths  $\sigma_{\pm\nu}$  which determines the reflection amplitude is easily calculated

$$\sigma_{\nu}\epsilon_{-\nu} + \sigma_{-\nu}\epsilon_{\nu} = 2\omega^2|\epsilon_{\nu}|^2\mathcal{C}^{(+)}\frac{W_0}{W_+W_-}, \quad W_0 = \eta_0 + k_x^2 + \nu^2K_g^2 + |\epsilon_{2\nu}|\cos\varphi_{\epsilon}\omega^2V. \quad (86)$$

This is the central result of this section. We will use it in the next section to analyze possible patterns of overlapping resonances.

## 2. Reflectivity of overlapping resonances

The equations (79) and (86) show that the zeros of the real parts of  $W_+$  and  $W_-$  define the positions of the two resonances while their widths are given respectively by  $\text{Im } W_+$  and  $\text{Im } W_-$ . According to Eq. (84) the sum of the resonance widths and the midpoint of their positions are not affected by the interaction of the resonances. It follows that broadening of one of the resonances is accompanied by narrowing of the other. This is reminiscent of the phenomenon of motional narrowing [39] as well as the phenomenon of superradiance [40] and subradiance [41] for coupled emitters. The distance  $|\text{Re}(W_+ - W_-)|$  between the two resonances can either shrink or expand depending on the structure of the GWS. If

$$\text{Re}\left((|\epsilon_{\nu}|^2\omega^2\Sigma - |\epsilon_{2\nu}|\cos\varphi_{\epsilon}V)^2 + |\epsilon_{2\nu}|^2\sin^2\varphi_{\epsilon}V^2\right) < 0, \quad (87)$$

and if the distance  $|4k_x\nu K_g|$  between the non-interacting resonances is sufficiently large this distance decreases due to the interaction. The condition (87) is actually satisfied for the choice of the parameters (58) where  $|\text{Im } \Sigma| \approx 2.5|\text{Re } \Sigma|$  and  $\epsilon_{2\nu} = 0$ . Obviously, for sufficiently large values of the term proportional to  $V$  repulsion of the resonances results. Below we will discuss such a case. For  $k_x = 0$  the distance trivially has to increase or to remain 0 as a consequence of the interaction. In the regime in between these limits the change in distance depends on the details of the various quantities in (87). It is remarkable that the system of overlapping resonances can be tuned to exhibit either “level” repulsion or attraction by variation of an external parameter ( $k_x$ ). A peculiarity of the interacting resonances is the appearance of a zero in the resonance amplitude, i.e.  $W_0(\omega, \theta) = 0$  in Eq. (86). The presence of this zero may distort significantly the shape of the reflectivity or obscure the presence of two resonances if the distance between the zero of  $W_0$  and the resonance position of  $W_-$  is of the same size as or smaller than the corresponding width.

Finally, the ratio of the kinematical term  $(2k_x\nu K_g)^2$  and the interaction induced 2nd term in the square root of Eq. (84) controls the transition from overlapping to isolated resonances. For sufficiently large  $k_x$  the interaction induced term, i.e. the off-diagonal matrix elements of  $W$  in (81) can be neglected and two isolated resonances are described by  $W$ .

We now will give a brief overview of the possible structures of the resonances generated by Eq. (86) and we will discuss their dependence on the properties of the GWS. In these qualitative studies, but not in the numerical results, we disregard the contribution  $r_0(\omega, k_x)$  to the reflection amplitude  $r(\omega, k_x)$  (cf. Eq. (79)). We first consider the case when  $|\epsilon_{2\nu}| = 0$  for which  $\varphi_{\epsilon_0}$  is ill defined. This is realized for a grating with 50% duty cycle. According to Eq. (84), for  $k_x \rightarrow 0$  the transition from two separated resonances to one resonance takes place. At  $k_x = 0$  only one resonance is present with a width twice as large as that of an isolated resonance ( $W_-$  is exactly canceled by  $W_0$ ), while at arbitrarily small non zero angles two peaks will appear due to the small imaginary part of  $W_-$ .

This is illustrated in the left part of Fig. 6 for the case where the resonance conditions are satisfied for modes with  $\nu = \pm 1$ . In the resonance region  $|\epsilon_1|^2 \omega^4 \Sigma \approx (0.07 + 0.16i) \mu\text{m}^{-2}$ . The distance between the resonances is thus smaller than the wide resonance width and indeed no clear separation of the resonances is observed until the incidence angle  $|\theta|$  is increased to values of the order of or larger than

$$|\theta| \geq -|\epsilon_1|^2 \omega^3 \text{Im } \Sigma / K_g \approx 0.3^\circ.$$

One can also see the effect caused by the zero of  $W_0$  in Eq. (86). It produces the dip in the combined peak in the left part of Fig. 6. The appearance of the zero can also be interpreted as arising from a cancelation between the contribution from the two eigenstates of  $W$  (81) associated with the eigenvalues  $W_\pm$ . This destructive interference of the contributions from the two eigenstates causes a transparency window within the resonance and is closely related to the ‘‘EIT’’ phenomenon (electromagnetically induced transparency), cf., Ref. [42]. Thus for an appropriate choice of parameters guided mode resonances provide yet another classical analog of EIT, cf., [43, 44].

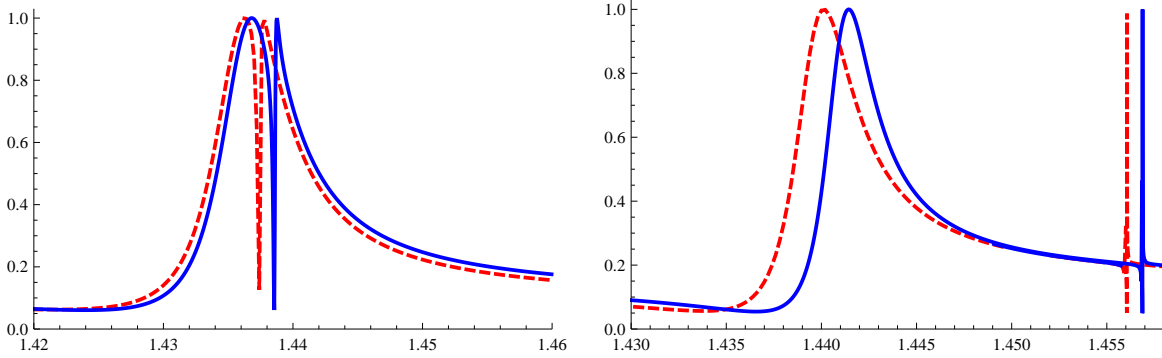


FIG. 6: Reflectivity as a function of the wavelength for the angle of incidence  $\theta = 0.05^\circ$ , structure and parameters as specified in Eqs. (57-58). Solid lines: exact values, dashed lines: values obtained in the resonance dominance approximation. Left: duty cycle  $d/\Lambda = 0.5$ . Right: duty cycle  $d/\Lambda = 0.75$ .

We now consider the case where  $\epsilon_{2\nu}$  and  $\epsilon_\nu^2$  are, up to a sign, in phase, i. e., for

$$\varphi_\epsilon = 0, \pi, \quad (88)$$

Then Eq. (84) simplifies for small  $k_x$ ,

$$W_\pm \approx \eta_0 + k_x^2 + \nu^2 K_g^2 + |\epsilon_\nu|^2 \omega^4 \Sigma \pm \left[ |\epsilon_\nu|^2 \omega^4 \Sigma - |\epsilon_{2\nu}| \omega^2 V + \frac{2k_x^2 \nu^2 K_g^2}{\omega^2 (|\epsilon_\nu|^2 \omega^2 \Sigma - |\epsilon_{2\nu}| \cos \varphi_\epsilon V)} \right]. \quad (89)$$

When the direct interaction  $V$  is strong in comparison to the self coupling  $\Sigma$  one will have a clear separation of the two resonances. Since  $V$  is real one of the resonances will still have a vanishing width at  $k_x = 0$  while another will have the full width. This is illustrated in the right part of Fig. 6 for the duty cycle of 75%. The shape of the reflectivity is drastically changed as compared to the left part of this figure showing two well separated resonances with widths which differ by a factor of 350.

It should be noted that any simple binary grating of arbitrary duty cycle (cf. left part of Fig (1)) are symmetric under x-mirror reflection over a plane defined by  $x = x_0$ . Any

grating with such symmetry will either have  $\epsilon_{2\nu} = 0$  or will fulfill the condition (88). Since the incident field is symmetric under x-mirror reflection symmetry only for  $k_x = 0$  we may interpret the vanishing width at normal incidence for such symmetric gratings as a symmetry selection rule. Thereby it is only possible to excite the combination of guided modes which is symmetric under the x-mirror reflection. Interacting resonances with similar widths at small or vanishing angle of incidence can be generated only if the relative phase  $\varphi_\epsilon$  (85) deviates significantly from 0 or  $\pi$ .

We consider the case

$$\varphi_\epsilon = \pm \frac{\pi}{2}. \quad (90)$$

and realize this value by choosing the profile of the grating shown in Fig. 7 with parameters

$$\Lambda = 0.81 \mu m, \quad \epsilon_{\min} = 1, \quad \epsilon_{\max} = 4, \quad d/\Lambda = 0.2. \quad (91)$$

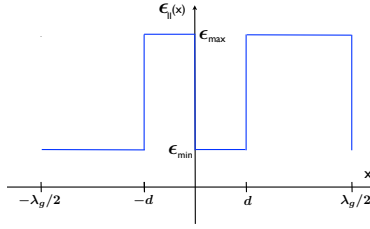


FIG. 7: Profile of the dielectric constant in an elementary interval of the grating layer with grating period  $\Lambda$ .

The structure of the resonance curves depend on the strength  $\alpha$  of the direct interaction of the 2 resonances in comparison to the indirect interaction via the extended mode

$$\alpha = \frac{|\epsilon_{2\nu}|V}{|\epsilon_\nu^2|\omega^2|\Sigma|}. \quad (92)$$

With the above choice of the parameters (91) the direct coupling dominates, i.e.  $\alpha \gg 1$ , and we find for small  $k_x$

$$W_\pm = \eta_0 + k_x^2 + \nu^2 K_g^2 + |\epsilon_\nu|^2 \omega^4 \Sigma \pm \left[ \omega^2 |\epsilon_{2\nu}| V + \frac{|\epsilon_\nu|^4 \omega^8 \Sigma^2 + 4k_x^2 \nu^2 K_g^2}{2\omega^2 |\epsilon_{2\nu}| V} \right]. \quad (93)$$

The direct interaction  $V$  generates a repulsion of the two resonances; to leading order in  $\alpha$ , their widths are equal that of a non-interacting resonances. Also in this limit the numerical results confirm our analytical analysis as is seen in Fig. 8.

### 3. Contour plots, band gaps and curvatures

Contour plots of the reflectivity in the  $\theta$ - $\lambda$  plane offer a convenient way to survey the scattering in different kinematical regimes including the separated and strongly interacting resonances. In Figs. (9) and (10) such contour plots are shown which correspond to structures and parameters of Figs. (6) and (8). Quantities which are important for applications and which can be extracted from the contour plots are the band gap, i.e. the difference in

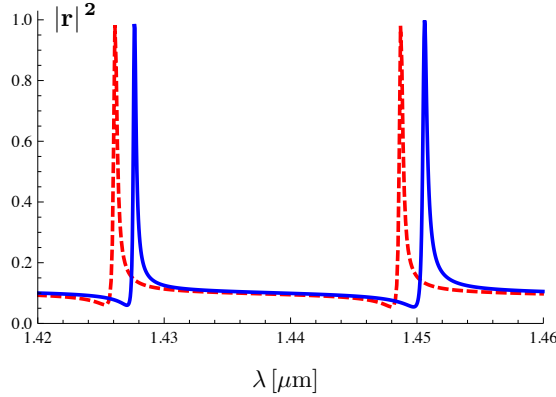


FIG. 8: Reflectivity as a function of the wavelength for the angle of incidence  $\theta = 0.005^\circ$ , grating structure shown in Fig. 7 and parameters (57), (58) and (91). Solid lines: exact values, dashed lines: values obtained in the resonance dominance approximation.

wavelength between the peaks  $|r|^2 = 1$  in the limit  $\theta \rightarrow 0$  and the curvature of the  $|r|^2 = 1$  curves at these points. We will calculate these quantities and establish their dependence on the parameters of the GWS.

An analytic understanding is possible only under the assumption that the coupling of extended and guided mode is weak, i.e.,  $|\epsilon_\nu \mathcal{C}^{(+)}|^2 \omega \ll 1$ . This condition is satisfied in all of the examples to be discussed. It implies that values of  $|r(\omega, k_x)|^2$  of the order of 1 can be realized only if  $\omega^2 |W_0/W_+ W_-| \gg 1$ , i.e. if  $\text{Re } W_+$  or  $\text{Re } W_- \approx 0$ . In the following analytical studies we therefore replace the contour lines of the reflectivity by the contour lines of the equations

$$\text{Re } W_\pm(\omega, \theta) \approx 0. \quad (94)$$

Fig. 10 displays the level repulsion arising from the direct coupling term in Eq. (93). We know from Fig. 6 that the strength of the level repulsion is correctly reproduced in resonance dominance. To calculate band gap and curvature we drop the sub leading terms proportional to  $\Sigma$  in Eq. (93), expand around  $\omega_0 = 2\pi/\lambda_0$ , the zero of  $\eta(\omega_0) + \nu^2 K_g^2$  and obtain the following expressions for the band gap  $\delta\lambda$  and curvature  $\kappa$

$$\delta\lambda \approx \frac{\lambda_0}{-\eta'_0} |\epsilon_{2\nu}| V, \quad \kappa = \frac{d\lambda}{d\theta^2} \approx \frac{\lambda_0}{-\eta'_0} \left( 1 \pm \frac{\nu^2 \lambda_0^2}{|\epsilon_{2\nu}| V \Lambda^2} \right), \quad -\eta'_0 = \left. \frac{d\eta_0(\omega^2)}{d\omega^2} \right|_{\omega^2=\omega_0^2}. \quad (95)$$

These estimates yield for the structure of Fig. 10  $\delta\lambda \approx 22$  nm, and for the curvature of the 2 contour lines  $\kappa \approx 0.3 \pm 6.8$  nm, and agree with the numerical results of Fig. 10.

Analytical results for the contour plot on the left hand side of Fig. 9 are harder to obtain due to the presence of the zero (cf. Fig. 6) of the resonance contribution to the reflection amplitude (cf. Eq. (86)) for the parameters (58) of the GWS. We note, that  $\epsilon_2 = 0$  for the choice of the duty cycle  $d/\Lambda = 1/2$ . As discussed above, the transition from isolated to interacting resonances takes place if

$$\left| \frac{\epsilon_1^2 \omega^4 \Sigma}{2\omega\theta K_g} \right| \approx 1. \quad (96)$$

With  $|\epsilon_1|^2 \omega^4 \Sigma \approx (0.06 + i0.16) \mu\text{m}^{-2}$  this condition is satisfied for  $\theta = 0.15^\circ$ . For larger values of  $\theta$  we expect a linear dependence of the wavelength on the angle of the incident light in

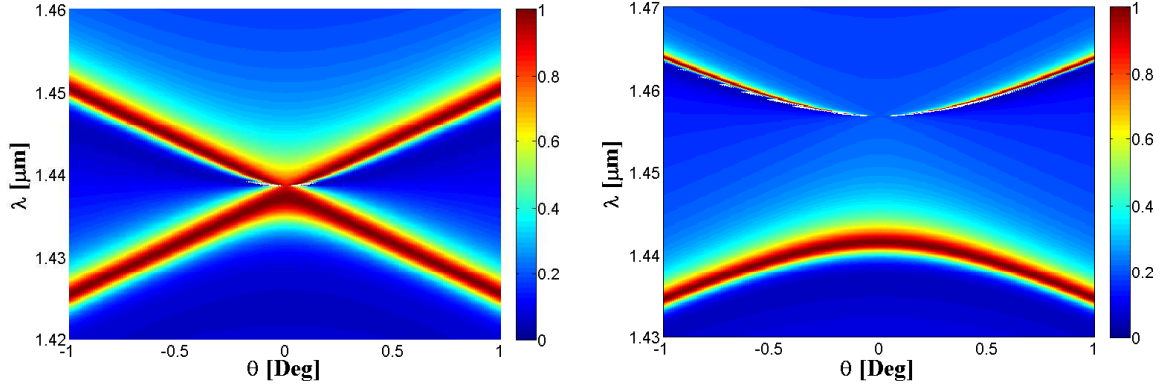


FIG. 9: Contour lines of the reflectivity in the  $\theta$ - $\lambda$  plane. Structure and parameters are specified in Eqs. (57-58). In the right part of the figure the duty cycle has been changed from 50 % to 75%

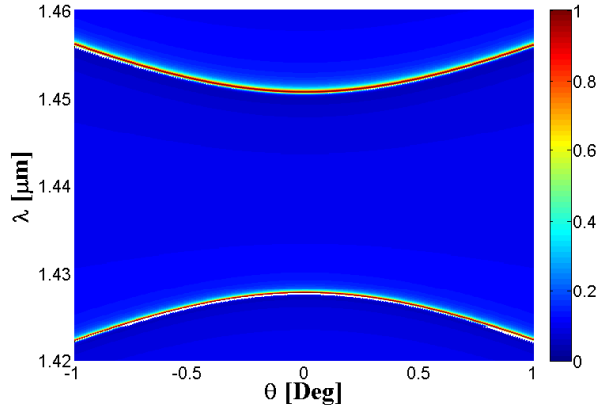


FIG. 10: Contour lines of the reflectivity in the  $\theta$ - $\lambda$  plane. Structure and parameters are specified in Eqs. (57), (58) and (91).

agreement with the numerical results. For significantly smaller values of  $\theta$  we consider the resonance associated with  $W_+$  which is not directly affected by the presence of the zero of  $W_0$ . We identify the lower branch of the contour lines of the reflectivity with the contour lines  $\text{Re } W_+ = 0$ . Expanding as above  $W_+$  around  $\omega_0$  we obtain

$$\kappa \approx -\frac{\lambda_0}{\eta'_0} \left( 1 - \text{Re} \frac{2K_g^2}{|\epsilon_1|^2 \omega_0^4 \Sigma} \right) \approx 110 \text{ nm}, \quad (97)$$

i.e., these estimates account for the order of magnitude difference of the curvatures in Fig. 10 and the left part of Fig. 9.

#### 4. Electric fields of overlapping resonances

So far, we have concentrated our discussion on one observable, the reflectivity. An independent observable is the resonating electric field with components  $E_{\pm\nu}$  (cf. Eq.(78)). With



only minor modifications the above analysis of the reflectivity can be applied. In terms of  $\sigma_{\pm}$ , the guided mode part of the electric field is given by (cf. Eq.)

$$E_{\nu}(x, z) + E_{-\nu}(x, z) = -i \left( e_{+} \cos \nu K_g x + e_{-} \sin \nu K_g x \right) e^{ik_x x} \mathcal{E}_{\eta_0}(z), \quad (98)$$

with

$$e_{+} = i(\sigma_{\nu} + \sigma_{-\nu}), \quad e_{-} = \sigma_{\nu} - \sigma_{-\nu}. \quad (99)$$

The calculation of the two components via Eqs. (80) and (83) is simplified if we choose  $\epsilon_{\nu}$  to be real (which always can be achieved with an appropriate choice of the origin of  $x$  in the integral (6)). It follows immediately from Eqs. (86) and (79) that  $e_{+}$  is proportional to the resonating part of the reflection amplitude

$$e_{+} = \frac{2i\epsilon_{\nu}\omega^2\mathcal{C}^{(+)}W_0}{W_{+}W_{-}} = -\frac{2k_z^{-}(r(\omega, k_x) - r_0(\omega, k_x))}{\epsilon_{\nu}\omega^2\mathcal{C}^{(+)}} \quad (100)$$

This expression is valid for any value of  $\theta$ . It applies also to the case of isolated resonances. Up to the normalization, the coefficient  $e_{+}$  is given by the (resonating part of the) reflection amplitude. As seen in Fig. 11,  $e_{+}$  vanishes at  $\omega_0$  and exhibits the same asymmetry around the corresponding wavelength as the reflectivity in Fig. 6. The absolute value of  $e_{+}$  is related to the half width of the isolated resonances (cf. Eq. 53) by

$$|e_{+}| = 2\sqrt{k_z^{-}/\tilde{\Gamma}} |r(\omega, k_x) - r_0(\omega, k_x)|, \quad (101)$$

i.e. the strength of this component of the electric field increases with decreasing half width  $\tilde{\Gamma}$ . In region III of the GWS (Fig. 1), the strength of the electric field proportional to  $e_{+}$  can be larger than the incident field by up to a factor of 10 (cf. Fig. 3). The  $e_{-}$ -component

$$e_{-} = \frac{2\epsilon_{\nu}\omega^2\mathcal{C}^{(+)}}{W_{+}W_{-}} (-2k_x\nu K_g + i|\epsilon_{2\nu}|\omega^2 V \sin \varphi_{\epsilon}) \quad (102)$$

of the resonating electric field differs from  $e_{+}$  by the factor  $W_0^{-1}$ . For

$$\varphi = 0, \pi$$

the appearance of  $W_0$  in Eq. (86) is necessary to keep the reflection amplitude finite by canceling the zero of  $W_{-}$  (cf. Eq. (89)). In turn this implies that  $e_{-}$  is singular for  $\theta \rightarrow 0$  and  $\omega = \omega_0$  where  $\omega_0$  denotes zero of  $W_0$

$$W_0(\omega_0) = \eta_0(\omega_0^2) + \nu^2 K_g^2 + \omega_0^2 |\epsilon_{2\nu}| V(\omega_0^2) = 0. \quad (103)$$

For values of  $(\theta, \omega^2)$  sufficiently close to the singular point  $(0, \omega_0^2)$  in the  $\theta, \omega^2$  plane,  $e_{-}$  is given by

$$e_{-} = \frac{4\omega_0\epsilon_{\nu}\mathcal{C}^{(+)}}{\nu K_g} \frac{\theta \Sigma_{-}}{\omega - \omega_0 + \theta^2 \Sigma_{-}}, \quad \Sigma_{-} = \frac{2\nu^2 K_g^2}{W_0'(\omega_0) \left( -|\epsilon_{\nu}|^2 \omega_0^2 \Sigma(\omega_0) + |\epsilon_{2\nu}| V(\omega_0^2) \right)}. \quad (104)$$

Considered as a function of  $\omega$ , for fixed  $\theta$ , the component  $e_{-}$  has a Lorentzian (Breit Wigner) shape. It reaches its maximal value at  $\omega = \omega_0 - \theta^2 \text{Re}\Sigma_{-}$

$$|e_{-}|_{\max} = \frac{4\sqrt{\tilde{\Gamma}k_z^{-}}}{|\nu|\omega_0 K_g \theta} \frac{|\Sigma_{-}|}{|\text{Im}\Sigma_{-}|}. \quad (105)$$

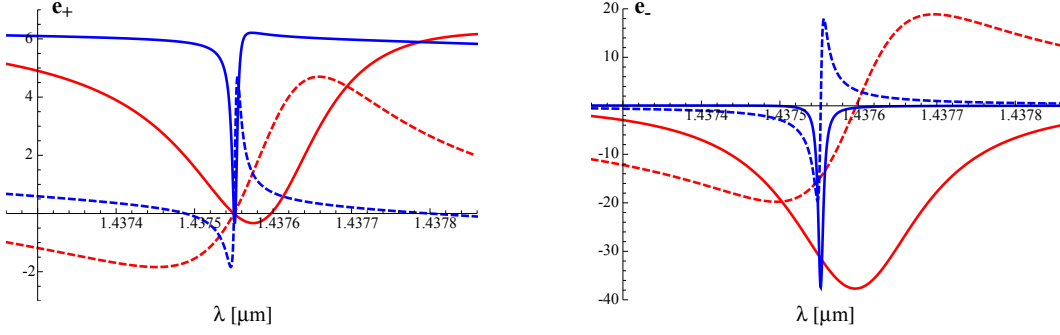


FIG. 11: Electric fields  $e_+$  (left) and  $e_-$  (right) (cf. Eqs. (100) and (102)) in units of the amplitude of the incident field as a function of the wavelength for the interacting resonances of the left hand side of Fig. 6. Solid lines: real part, dashed lines: imaginary part, red (color online)  $\theta = 0.05^\circ$ , blue (color online)  $\theta = 0.01^\circ$ . The values for  $e_-$  at  $\theta = 0.01^\circ$  have been divided by a factor of 5.

As Fig. 11 demonstrates the increase in the electric field strength with decreasing angle  $\theta$  of the incident light is accompanied by a decrease of the half width  $\theta^2 \text{Im} \Sigma_-$  of the Breit-Wigner function (104). In the homogeneous layer III (cf., Figs. 1, 3) the resonating part of the electric field reaches values which are up to a factor  $3/\theta[^\circ]$  larger than the field of the incident light.

## B. Overlapping TM resonances

### 1. Formal development

We now consider interacting resonances in the TM case. We follow the developments in Section IV and consider the case when there are two eigenvalues  $\eta_1 \equiv \eta_{n_1, \nu_1}$  and  $\eta_2 \equiv \eta_{n_2, \nu_2}$  with values close to  $\omega^2$ . As the comparison of Eqs. (16) and (38) shows, unlike in the TE case, the guided modes  $\mathcal{H}_{n, \nu_i}$  depend on the index  $n$  which makes the following analysis more involved. The same complications will occur in the TE case if overlapping resonances associated with different eigenvalues  $\eta_{n_{1,2}}$  are considered.

We retain both resonating terms in the system of equations (40) and write coupled equations for the resonating and the zero components. We will then use the resonance dominance approximation retaining only a single term with the guided mode  $\mathcal{H}_{n_i, \nu_i}(z)$  in the sums over  $i$  in Eq.(42)

$$H_0(z) = H_0^{(+)}(z) + \int_{I_g} dz' g(z, z') (\Theta_{0, n_1} H_{n_1}(z') + \Theta_{0, n_2} H_{n_2}(z')) , \quad (106)$$

$$H_{n_1}(z) = \frac{1}{\omega^2 - \eta_1} \mathcal{H}_{n_1, \nu_1}(z) \int_{I_g} dz' \mathcal{H}_{n_1, \nu_1}(z') (\Theta_{n_1, 0} H_0(z') + \Theta_{n_1, n_2} H_{n_2}(z')) , \quad (107)$$

$$H_{n_2}(z) = \frac{1}{\omega^2 - \eta_2} \mathcal{H}_{n_2, \nu_2}(z) \int_{I_g} dz' \mathcal{H}_{n_2, \nu_2}(z') (\Theta_{n_2, 0} H_0(z') + \Theta_{n_2, n_1} H_{n_1}(z')) . \quad (108)$$

As in the case of the single resonance the components  $H_{n_1}$  and  $H_{n_2}$  are proportional to the guided modes

$$H_{n_1}(z) = \sigma_{n_1} \mathcal{H}_{n_1, \nu_1}(z) , \quad H_{n_2}(z) = \sigma_{n_2} \mathcal{H}_{n_2, \nu_2}(z) , \quad (109)$$

but the equations determining  $\sigma_{n_i}$ 's show mixing of the two resonating modes. Inserting (109) into (107) and (108) together with (106) we obtain closed equations for the field enhancement coefficients

$$W \begin{pmatrix} \sigma_{n_1} \\ \sigma_{n_2} \end{pmatrix} = \begin{pmatrix} \gamma_{n_1} \mathcal{C}_{n_1}^{(+)} \\ \gamma_{n_2} \mathcal{C}_{n_2}^{(+)} \end{pmatrix} \quad (110)$$

where, in analogy with the TE case (Eqs. (80), (81), we have introduced the coupling matrix

$$W = \begin{bmatrix} \omega^2 - \mu_1 & -\gamma_{n_1-n_2}V - \gamma_{n_1}\gamma_{-n_2}\Sigma_{n_1,n_2} \\ -\gamma_{n_2-n_1}V - \gamma_{-n_1}\gamma_{n_2}\Sigma_{n_2,n_1} & \omega^2 - \mu_2 \end{bmatrix}, \quad (111)$$

and

$$\mu_i = \eta_i + |\gamma_{n_i}|^2 \Sigma_{n_i, n_i}. \quad (112)$$

We have used the replacement explained in Appendix VI C  $\Theta_{nm} \rightarrow \gamma_{n-m} \tilde{\Theta}_{nm}$  with the notation

$$\tilde{\Theta}_{nm} = \overleftarrow{\partial}_z \overrightarrow{\partial}_z + (k_x + nK_g)(k_x + mK_g). \quad (113)$$

The quantities

$$\mathcal{C}_{n_i}^{(+)} = \int_{I_g} dz' \mathcal{H}_{n_i, \nu_i}(z') \tilde{\Theta}_{n_1, 0} H_0^{(+)}(z'), \quad (114)$$

$$\Sigma_{n_i, n_j} = \int_{I_g} dz' \int_{I_g} dz'' \mathcal{H}_{n_i, \nu_i}(z') \tilde{\Theta}_{n_i, 0} g_0(z', z'') \tilde{\Theta}_{0, n_j} \mathcal{H}_{n_j, \nu_j}(z''), \quad i, j = 1, 2. \quad (115)$$

are generalizations of the definitions (71) and (72) for isolated resonances. Here a new quantity appears

$$V = \int_{I_g} dz' \mathcal{H}_{n_1, \nu_1}(z') \tilde{\Theta}_{n_1, n_2} \mathcal{H}_{n_2, \nu_2}(z') \quad (116)$$

which controls the direct coupling between the two guided modes. An indirect coupling between the guided modes via the interaction with the extended mode is generated by  $\Sigma_{n_1, n_2} = \Sigma_{n_2, n_1}$ . The quantities  $\Sigma_{n_i, n_i}$  are the self-interactions of each guided mode via the extended mode. Note that for the dielectric structure in which  $\gamma_{n_1} = \gamma_{n_2} = 0$  but with  $\gamma_{n_1-n_2} \neq 0$  we obtain the standard avoided level crossing problem, i.e. the non radiating photonic band gap case.

The eigenvalues of  $W$  and the field enhancement coefficients are given by

$$W_{\pm} = \omega^2 - (\mu_1 + \mu_2)/2 \pm \sqrt{(\mu_1 - \mu_2)^2/4 + (\gamma_{n_1-n_2}V + \gamma_{n_1}\gamma_{-n_2}\Sigma_{n_1,n_2})(\gamma_{n_2-n_1}V + \gamma_{-n_1}\gamma_{n_2}\Sigma_{n_2,n_1})}, \quad (117)$$

$$\sigma_{n_1} = \frac{\gamma_{n_1}(\omega^2 - \mu_2)\mathcal{C}_{n_1}^{(+)} + \gamma_{n_2}(\gamma_{n_1-n_2}V + \gamma_{n_1}\gamma_{-n_2}\Sigma_{n_1,n_2})\mathcal{C}_{n_2}^{(+)}}{W_+ W_-}, \quad (118)$$

$$\sigma_{n_2} = \frac{\gamma_{n_1}(\gamma_{n_2-n_1}V + \gamma_{-n_1}\gamma_{n_2}\Sigma_{n_2,n_1})\mathcal{C}_{n_1}^{(+)} + \gamma_{n_2}(\omega^2 - \mu_1)\mathcal{C}_{n_2}^{(+)}}{W_+ W_-}. \quad (119)$$

Using Eq. (106) and the asymptotics of the Green's function (cf. Appendix VI B) the reflection amplitude is given by

$$r(\omega, k_x) = r_0(\omega, k_x) - \frac{i\epsilon_I}{2k_z^-} (\sigma_{n_1}\gamma_{-n_1}\mathcal{C}_{n_1}^{(+)} + \sigma_{n_2}\gamma_{-n_2}\mathcal{C}_{n_2}^{(+)}) \quad (120)$$

## 2. Overlapping resonances close to normal incidence.

To proceed with the analysis we now specify to the special case of the vicinity of  $k_x = 0$ . We note that a solution of Eq. (39) with a given  $k_x$  and  $n$  is also a solution with  $k_x \rightarrow -k_x$  and  $n \rightarrow -n$ . This means that at  $k_x = 0$  the resonance condition (43) will always be satisfied by a pair of guided modes. Let us consider such a resonating pair with the eigenvalues  $\eta_{n,\nu} = \eta_{-n,\nu}$ . For such a pair  $n_1 = n = -n_2$  and at  $k_x = 0$  all the components of  $\mathcal{C}^{(+)}$  and of  $\Sigma$  are identical and given by

$$\begin{aligned}\mathcal{C}^{(+)} &= \mathcal{C}_{n_i}^{(+)} = \int_{I_g} dz' [\partial_{z'} \mathcal{H}_{n,\nu}(z')] [\partial_{z'} H_0^{(+)}(z')] , \\ \Sigma &= \Sigma_{n_i, n_j} = \int_{I_g} dz' dz'' [\partial_{z'} \mathcal{H}_{n,\nu}(z')] [\partial_{z'} \partial_{z''} g_0(z', z'')] [\partial_{z''} \mathcal{H}_{n,\nu}(z'')] , \\ V &= \int_{I_g} dz' \{ [\partial_{z'} \mathcal{H}_{n,\nu}(z')]^2 - (nK_g)^2 [\mathcal{H}_{n,\nu}(z')]^2 \} .\end{aligned}\tag{121}$$

For small deviations from  $k_x = 0$  we find

$$\Delta\eta_{\pm n,\nu} = \pm 2\zeta n K_g k_x, \quad \zeta = \int_{-\infty}^{\infty} dz \gamma_0(z) \mathcal{H}_{n,\nu}^2(z), \tag{122}$$

where we have used Eq. (38) and

$$\frac{\partial \eta_{n\nu}}{\partial k_x} = \int_{-\infty}^{\infty} dz \mathcal{H}_{n,\nu} \frac{\partial \Theta_{nn}}{\partial k_x} \mathcal{H}_{n,\nu}. \tag{123}$$

Identifying for simplicity  $\Sigma$  and  $V$  with their values at  $k_x = 0$ , we approximate Eq. (117) by

$$\begin{aligned}W_{\pm} &= [\omega^2 - \eta_{n,\nu} - |\gamma_n|^2 \Sigma] \\ &\pm \sqrt{(2\zeta k_x n K_g)^2 + (|\gamma_n|^2 \Sigma^2 + |\gamma_{2n}| \cos \varphi_{\gamma} V)^2 + |\gamma_{2n}|^2 \sin^2 \varphi_{\gamma} V^2}\end{aligned}\tag{124}$$

with

$$e^{i\varphi_{\gamma}} = \frac{\gamma_{2n} \gamma_n^{\star 2}}{|\gamma_{2n} \gamma_n^2|}. \tag{125}$$

The reflection amplitude is given by

$$r(\omega, k_x) = r_0(\omega, k_x) - \frac{i\epsilon_I |\gamma_n|^2 (\mathcal{C}^{(+)})^2}{k_z} \frac{W_0}{W_+ W_-}, \quad W_0 = \omega^2 - \eta_{n,\nu} + |\gamma_{2n}| \cos \varphi_{\gamma} V. \tag{126}$$

The above expressions for  $W_{\pm}$  and  $r(\omega, k_x)$  have the same form as in the TE case (cf. Eqs. (84), (86)). We again find that the interference of the contributions of the two eigenvalues  $W_{\pm}$  of the matrix  $W$  gives rise to a zero in the resonance part of the reflection amplitude. Also the role played by the phase  $\varphi_{\gamma}$  is identical to that of the TE phase  $\varphi_{\epsilon}$ . In particular for values

$$\varphi = 0, \pi$$

the width of one of the resonances (corresponding to  $W_+$ ) goes to zero at  $k_x = 0$ . This is illustrated in Fig. 12. In Figs. 13 we show an example of resonance dominance compared to the exact results.

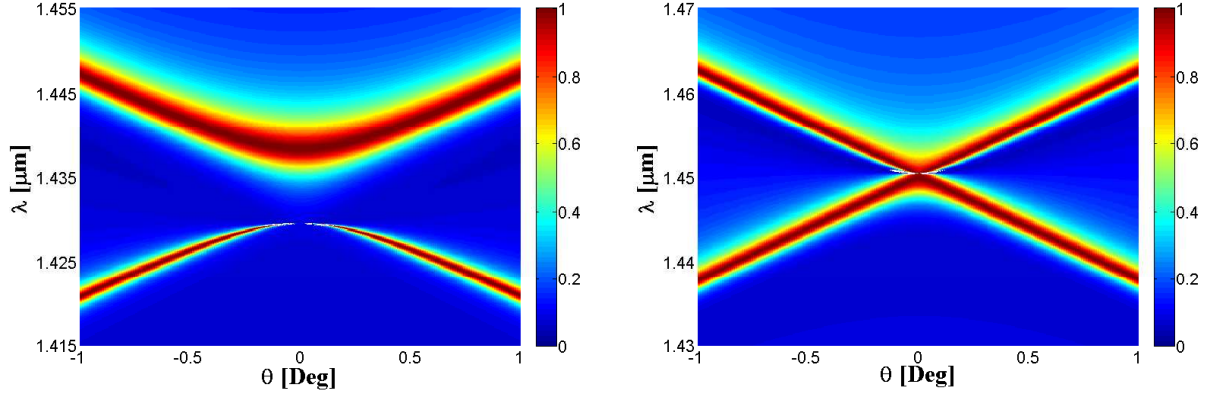


FIG. 12: Contour lines (exact results) of the reflectivity for TM polarization in the  $\theta$ - $\lambda$  plane. Structure and parameters as given in Eqs. (57-58) apart of the grating period  $0.87\mu m$  and 50% duty cycle (left figure), 75% duty cycle (right figure).

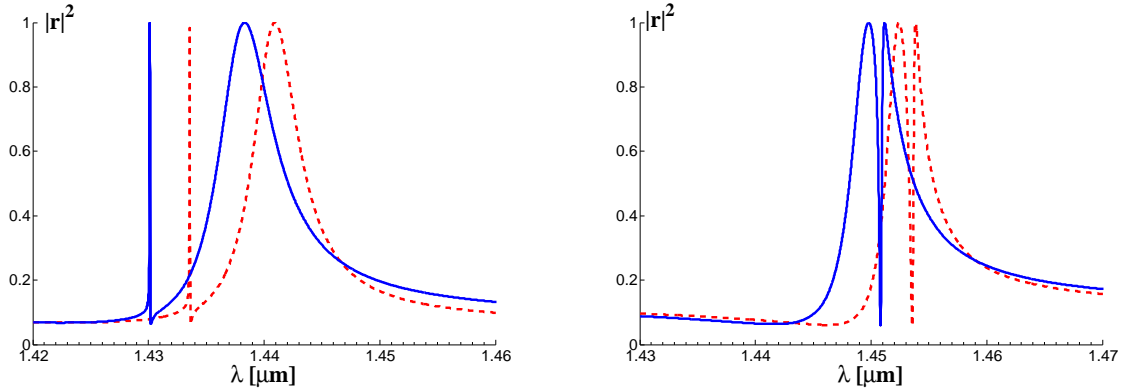


FIG. 13: Reflectivity for TM polarization as a function of the wavelength at  $\theta = 0.05^\circ$  for the same structure and parameters as in Fig. 12 with 50% duty cycle (left figure), 75% duty cycle (right figure). Solid lines: exact values (vertical cut in Fig. 12), dashed lines: resonance dominance approximation (cf., Eq.(125) with  $\varphi_\gamma = 0$ ).

Note that the dependence on the duty cycle of the TM results is qualitatively very different from the TE case, Figs. 6 and 9. The apparent band gap at  $k_x = 0$  closes at a very different value of the duty cycle. The source of this difference is clearly seen in our theory. Let us define the band gap as the difference between the two resonant frequencies at normal incidence. This corresponds to the difference between the real parts of  $W_+$  and  $W_-$ . When the band gap size is significantly larger than the FWHM of the wider of the two resonances, the two resonances are well separated and thus the band gap becomes clearly visibly as in the left part of Fig. 12. For the band gap of the order or smaller than the wider resonance width the resonances overlap and appear merged.

According to Eq. (84) and (125) the difference between  $W_+$  and  $W_-$  for  $\varphi = 0, \pi$  is given by

$$2\omega^2 (|\epsilon_\nu|^2 \omega^2 \Sigma + |\epsilon_{2\nu}|V) \quad \text{and} \quad 2(|\gamma_n|^2 \Sigma + |\gamma_{2n}|V) \quad (127)$$

for TE and TM respectively. When the duty cycle is close to 50% we have vanishing  $|\epsilon_{2\nu}|$  so that the direct coupling term  $V$  does not contribute in the TE case. At the same time  $\gamma_{2n}$  does not vanish in the inverse Fourier transform matrix approach which we adopted as explained in Section III B. This difference between the TE and TM is however not as important as the difference in the expressions for  $\Sigma$ . They are respectively given by Eqs. (52) and (121) with the reference to expressions (149) and (169). Comparing we notice a peculiar term present only in the TM case. This is the last term in (169). It is proportional to the  $\delta$ -function and produces a "contact" term

$$-1/\gamma_0 \int_{I_g} dz' [\partial_{z'} \mathcal{H}_{n,\nu}(z')]^2 \quad (128)$$

in the expression for  $\Sigma$  in the TM case. We call this term "contact" since in it the mode functions  $\partial_z \mathcal{H}_{n,\nu}(z)$  "interact" at one point. This is in contrast to expression (84) for the TE or (125) with only the first term of (169) for TM. In those cases the mode functions interact via a finite range interaction caused by the propagation in the extended mode.

The contact term is real and therefore contributes to the band gap. Numerical evidence shows that this is the dominant contribution for the 50% duty cycle and is significantly larger than the wider resonance width given by the imaginary part of  $\Sigma$ . This is the reason the apparent band gap is present at this duty cycle in the TM case. In order to complete the argument and to understand why the real part of  $\Sigma$  does not give rise to the same effect, we also compare the corresponding quantities for TE and TM case. To estimate the above contribution to the TM  $\text{Re}\Sigma$  we write in the thin grating case

$$|\gamma_n|^2 \int_{I_g} dz' [\partial_{z'} \mathcal{H}_{n,\nu}(z')]^2 \approx |\gamma_n|^2 \ell_g \mathcal{H}_{n,\nu}'^2(\ell_g/2).$$

We compare this estimate with the corresponding TE result

$$|\epsilon_\nu|^2 \omega^4 \text{Re}\Sigma \approx \frac{1}{6} |\epsilon_\nu|^2 \omega^4 \ell_g^3 \mathcal{E}_{\eta_0}^2(\ell_g/2)$$

recalling also that we have to divide the TE result by  $d\eta_0/d\omega^2 \approx 3.5$  before we can interpret it as a shift.

As one changes to higher or lower values of the duty cycle the second term, the direct interaction  $V$  begins to play a role in Eq. (127). Here again the explicit expressions of  $V$ , cf., (82) and (121) show the clear difference between the TE and the TM waves. In the former  $V$  is real, positive and therefore contributes to the increase of the band gap. For the TM case  $V$  is a difference of two positive terms and can be either positive, i.e. increasing the gap or negative, i.e. leading to its decrease. In fact we find that the apparent TM band gap closes at 75% duty cycle, cf. the right part of Fig. 12 as well as at 17 %, unlike in the TE case where the band gap closes only for a single value of the duty cycle.

The overall agreement between the resonance dominance and the exact results in the TM case is not as satisfactory as for the TE case. As an example we show in Fig. 14 the TM results for the same complex grating as in the TE case, cf., Fig. 7 and Eq. (91) with  $\lambda_g = 0.87\mu m$ . It is seen that the band gap is significantly smaller and the relative widths of the two resonances are different in the resonance dominance approximation as compared to the exact results. In our understanding there is a number of effects in the TM case contributing to such a discrepancy vis-a-vis an excellent agreement which is obtained in the

TE case. Firstly, it is known, cf., Ref. [33] that numerical convergence as a function of number of truncation orders is much slower in the TM case than the TE case. We note that the grating parameters as in Eq. (91) lead to  $|\gamma_2| \gg |\gamma_1|$  raising the relative importance of the higher order components.

Secondly, we believe that the issue of the special boundary conditions (cf., the end of Section III B) in the TM case is not accounted properly in our way of implementing the resonance dominance approximation. We plan to address this and related problems of the TM polarized scattering in the future work.

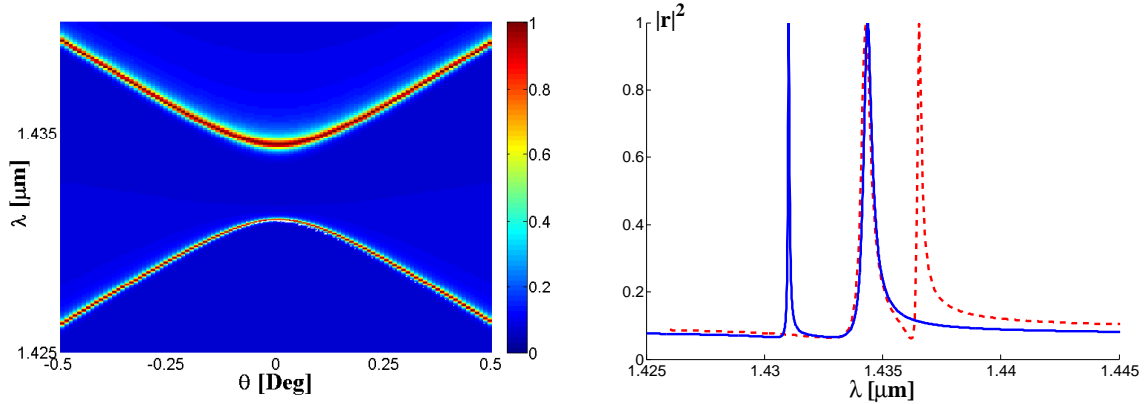


FIG. 14: Left: contour lines (exact results) of the reflectivity for TM polarization in the  $\theta$ - $\lambda$ . Right: reflectivity for TM polarization as a function of the wavelength at  $\theta = 0.005^\circ$ . Solid line: exact values (vertical cut in the left figure), dashed line: resonance dominance approximation (cf., Eq.(125). Same structure and parameters as in Fig. 12 apart the grating parameters which are given by Eq. (91) with  $\lambda_g = 0.87\mu m$ .

### C. Comparison with coupled resonances in quantum mechanics

The physics of coupled guided mode resonances of light scattering off photonic crystal slabs discussed above is closely related to the physics of interacting (overlapping) resonances or bound states in quantum mechanics. This connection is obvious in the limit of vanishing coupling  $\epsilon_\nu$  to the extended mode. Then the matrix  $W$  (81) is hermitian and the two (real) eigenvalues  $W_\pm$  of  $W$  can be written as

$$W_\pm = \frac{1}{2} [W_1 + W_2 \pm \sqrt{(W_1 - W_2)^2 + 4\omega^4 |\epsilon_{2\nu}|^2 V^2}], \quad W_{1,2} = \eta_0 + (k_x \pm \nu K_g)^2. \quad (129)$$

It's counterpart is the quantum mechanical two level system defined by the Hamiltonian matrix

$$H = \begin{pmatrix} E_1 & v \\ v & E_2 \end{pmatrix}, \quad (130)$$

with the energy eigenvalues  $E_\pm$

$$E_\pm = \frac{1}{2} (E_1 + E_2 \pm \sqrt{(E_1 - E_2)^2 + 4v^2}). \quad (131)$$

The level repulsion, i.e., increase of the gap of the two eigenvalues with increasing  $v^2$  or  $V^2$  is the characteristic property of both systems. To establish the correspondence in the general case is more involved since the matrix  $W$  (81) is not hermitian. The non-hermitian contribution arises due to the non-vanishing imaginary part of  $\Sigma$ . The (identical) contributions of  $\text{Im}(\Sigma)$  to the diagonal elements of  $W$  is due to the decay into the extended mode. Similarly the imaginary part of the off diagonal elements, i.e., in the coupling between the  $m = \pm\nu$  modes,  $\Sigma$  appears since this coupling is generated by intermediate excitation of the extended mode. Nevertheless  $W$  is not a general complex matrix. The conservation of flux restricts the non-hermitian part. Separating hermitian and non-hermitian contributions

$$W = W_h - iW_{nh},$$

one easily verifies that the non-hermitian part possesses the following structure

$$W_{nh} = w^\dagger w,$$

with

$$w = \omega^2 \sqrt{\text{Im}\Sigma} \begin{pmatrix} 0 & 0 \\ \epsilon_{-\nu} & \epsilon_\nu \end{pmatrix},$$

In quantum mechanical scattering on many body systems such as nuclei or atoms, the effective Hamiltonian whose eigenvalues are given by the resonance positions and widths exhibits exactly this structure of its non-hermitian part [3], [45], [46].

## V. CONCLUSION

The focus of our studies has been on the nature and the properties of resonances which are generated in scattering of light off photonic crystal slabs. We have established that these resonances are Feshbach resonances, i.e., they are the optical analog of a particular type of resonances formed in quantum mechanical scattering of particles off atoms or atomic nuclei. In quantum mechanics, bound states of many body systems in the absence of the coupling to the projectile are the progenitors of the resonances. In classical optics the role of the progenitors is played by the guided modes of the dielectric slabs in the absence of the coupling to the extended modes where the grating region is replaced by a homogeneous layer with an effective dielectric constant. Turning on the respective couplings, bound states and guided modes are converted into resonances. Close to the resonance, the interaction between projectile and target is dominated by resonance formation. We have shown in our investigations that resonance dominance is not only an important concept but also a quantitative tool in the analysis of scattering of light off photonic crystal slabs.

In the formal part of our studies we have employed techniques developed in the context of nuclear reactions to establish the resonances observed in scattering of light off photonic crystal slabs as Feshbach resonances. Despite of the common framework of resonance dominance we have identified significant differences in the implementation for TE and TM polarizations. We have derived expressions for the observables, the reflection and transmission amplitudes and the strengths of the magnetic and electric fields. The various shapes of the reflectivity as function of the wave length are properly reproduced. Also strong distortions of the Breit-Wigner form are correctly described in resonance dominance and shown to result from the interference between background scattering and resonance formation. In comparison



with results of exact numerical evaluations the accuracy of resonance dominance has been established to range, depending on the particular application, from a few to 15 % .

In comparison with exact numerical methods, the power of the resonance dominance approach rests upon the analytical formulation of the observables. It offers the possibility to study in detail the dependence of reflection and transmission amplitudes and the strength of the electromagnetic fields in terms of the properties of photonic crystal slabs and the kinematics of the incident light. We have demonstrated this potential of resonance dominance in the analysis of the rather involved phenomena appearing in the excitation of interacting resonances. In particular, we have been able to identify the source for the significant differences in the interaction of TE and TM resonances and the relevant parameters of the grating layer which control the shape of the reflectivity of overlapping resonances. We have derived analytical expressions for the band gap and the related curvature as a function of the angle of incidence and have study analytically the weird behavior of the electromagnetic field enhanced by the overlapping resonances. Needless to say that for design issues this analytical procedure can be reversed, i.e. the properties of the photonic crystal slabs can be identified which optimize certain requirements on observables.

## VI. APPENDICES

### A. Feshbach projection operators for light scattering

Since Feshbach's seminal work [1–3] on the theory of nuclear reactions, the main tool for such investigations is the formulation in terms of projection operators acting in an appropriately defined Hilbert space. We now will sketch a reformulation of this approach in the context of differential equations describing the classical scattering of light, [4, 16, 47].

We will first consider the TE case. It is convenient to begin with the coupled equations (10). We will rewrite them in the form

$$\sum_{m=-\infty}^{\infty} [-\partial_z^2 + (k_x + nK_g)(k_x + mK_g)]\delta_{nm} + \omega^2(\delta_{nm} - \epsilon_{m-n}(z))E_m(z) = \omega^2 E_n(z) \quad (132)$$

or in the matrix-operator notation

$$h\psi = \omega^2\psi \quad (133)$$

where

$$h_{nm} = [-\partial_z^2 + (k_x + nK_g)(k_x + mK_g)]\delta_{nm} + \omega^2(\delta_{nm} - \epsilon_{m-n}(z)) \quad (134)$$

and

$$\psi(z) \equiv \{..., E_{-m}(z), ..., E_{-1}(z), E_0(z), E_1(z), ..., E_m(z), ...\} \quad (135)$$

We define projection operators acting on the array  $\psi(z)$

$$\begin{aligned} P\psi &\equiv \psi_P = \text{array obtained from } \psi \text{ by setting to zero all components apart of } \psi_0, \\ Q\psi &\equiv \psi_Q = \text{array with the same components as } \psi \text{ but with } \psi_0 = 0 \end{aligned} \quad (136)$$

Clearly

$$P^2 = P, \quad Q^2 = Q, \quad P + Q = 1 \quad (137)$$

In a way which is standard in the Feshbach formalism [1],[3] we can act with  $P$  and with  $Q$  on our basic equation  $h\psi = \omega^2\psi$ . Using the above properties of  $P$  and  $Q$  we obtain coupled equations of the Feshbach formalism

$$\begin{aligned} h_{PP}\psi_P + h_{PQ}\psi_Q &= \omega^2\psi_P \\ h_{QQ}\psi_Q + h_{QP}\psi_P &= \omega^2\psi_Q \end{aligned} \quad (138)$$

where we defined

$$PHP = h_{PP} \ , \ QHQ = h_{QQ} \ , \ PhQ = h_{PQ} \ , \ QhP = h_{QP}.$$

Clearly  $h_{PP} = h_{00}$ ,  $h_{QQ}$  is the matrix  $h_{nm}$  with  $n = 0$  row and  $m = 0$  column excluded. The operators  $h_{PQ}$  and  $h_{QP}$  are matrices consisting respectively of just  $n = 0$  row and  $m = 0$  column both without the  $m = n = 0$  element. We can formally solve the second equation

$$\psi_Q = (\omega^2 - h_{QQ})^{-1}h_{QP}\psi_P \quad (139)$$

and insert into the first equation. Converting the resulting equation into an integral form we obtain

$$\begin{aligned} \psi_P(z) &= \psi_0^{(+)}(z) + \int dz' g_0(z, z') \langle z' | h_{PQ} | \psi_Q \rangle = \\ &= \psi_0^{(+)}(z) + \int dz' g_0(z, z') \langle z' | h_{PQ} (\omega^2 - h_{QQ})^{-1} h_{QP} | \psi_P \rangle \end{aligned} \quad (140)$$

where  $\psi_0^{(+)}$  is the properly chosen solution of  $(\omega^2 - h_{PP})\psi_0^{(+)} = 0$  and  $g_0(z, z')$  is the (properly chosen) Green's function of this equation, i.e.  $(\omega^2 - h_{PP})g_0 = 1$ . The meaning of "properly chosen" for the present problems is explained in Appendix VI B. We have also assumed that there is no unperturbed solution in the  $Q$  sector, i.e.  $\psi_Q = 0$  for  $h_{PQ} = 0$ .

So far we made no approximations. Let us consider the eigenfunctions of  $h_{QQ}$

$$h_{QQ}\phi_\nu = \tilde{\eta}_\nu\phi_\nu \quad (141)$$

and assume that the geometrical parameters of the optical system and the kinematics of the light scattering are such that there exist a range of discrete values of  $\tilde{\eta}_\nu$  (guiding modes). We will further assume that  $h_{PP}$  has a range of continuum eigenvalues (radiating modes) which overlap with the discrete modes of  $h_{QQ}$  and moreover that  $\omega^2$  lies within this combined range. In these circumstances the "off diagonal" terms  $h_{PQ}$  and  $h_{QP}$  couple the guiding modes to the radiating modes turning the former into Feshbach resonances. Note that we use  $\tilde{\eta}_\nu$  to distinguish from  $\eta_\nu$  used in the TE section of the main text.

A generalized version of the resonance dominance approximation used in the present work amounts to using one or few resonant terms in the full spectral decomposition Green's function in the  $Q$  sector

$$\frac{1}{\omega^2 - h_{QQ}} = \sum_\nu \frac{|\phi_\nu\rangle\langle\phi_\nu|}{\omega^2 - \tilde{\eta}_\nu} + G_c \quad (142)$$

where  $G_c$  is the contribution due to the continuum eigenfunctions. Using as an example two resonating eigenstates we obtain

$$\frac{1}{\omega^2 - h_{QQ}} \approx \frac{|\phi_1\rangle\langle\phi_1|}{\omega^2 - \tilde{\eta}_1} + \frac{|\phi_2\rangle\langle\phi_2|}{\omega^2 - \tilde{\eta}_2} \quad (143)$$

which means (cf., (139) that

$$\psi_Q = \sigma_1 \phi_1 + \sigma_2 \phi_2 \quad , \quad \sigma_i = (\omega^2 - \tilde{\eta}_i)^{-1} \langle \phi_i | h_{QP} | \psi_p \rangle \quad , \quad i = 1, 2 \quad (144)$$

Following the standard route one inserts this into (140)

$$\psi_P(z) = \psi_0^{(+)}(z) + \sum_{i=1,2} \sigma_i \int dz' g_0(z, z') \langle z' | h_{PQ} | \phi_i \rangle, \quad (145)$$

then multiplies and integrates by  $\int dz \langle \phi_j | h_{QP} | z \rangle \dots$  with  $j = 1$  and  $j = 2$  and obtains coupled equations for  $\sigma_i$

$$\begin{pmatrix} \omega^2 - \tilde{\eta}_1 - \Sigma_{11} & -\Sigma_{12} \\ -\Sigma_{21} & \omega^2 - \tilde{\eta}_2 - \Sigma_{22} \end{pmatrix} \begin{pmatrix} \sigma_1 \\ \sigma_2 \end{pmatrix} = \begin{pmatrix} \mathcal{C}_1^{(+)} \\ \mathcal{C}_2^{(+)} \end{pmatrix} \quad (146)$$

Here

$$\Sigma_{ij} = \langle \phi_i | h_{QP} g_0 h_{PQ} | \phi_j \rangle \quad , \quad \mathcal{C}_i^{(+)} = \langle \phi_i | h_{QP} | \psi_0^{(+)} \rangle \quad , \quad i = 1, 2 \quad (147)$$

In the TM scattering one can follow exactly the same route by simply noting that the basic set of equations (31) is already in the form  $h\psi = \omega^2\psi$  with  $h_{nm} \equiv \Theta_{nm}$  and

$$\psi(z) \equiv \{ \dots, H_{-m}(z), \dots, H_{-1}(z), H_0(z), H_1(z), \dots, H_m(z), \dots \} \quad (148)$$

It is important to recognize that equations (146) are based on assumed exact eigenfunctions  $\phi_1$  and  $\phi_2$  of  $h_{QQ}$ , Eq. (141). In reality  $h_{QQ}$  is almost as complicated as the full  $h$  in Eq. (134) and further approximations are required. In our treatment of overlapping resonances leading to (80) and (110) we have drastically truncated the problem and replaced the exact  $\phi_1$  and  $\phi_2$  by the eigenfunctions of  $h_{11}$  and  $h_{22}$ . In this way the coupling between these components via  $h_{12}$  and  $h_{21}$  as well as the coupling to other components are neglected. In fact we observe that equation (146) is similar in form to the equations (80) and (110) apart from the absence of the term  $V$  in the off diagonal elements of the matrix  $W$ . This term approximately accounts in Eqs. (80) and (110) for the direct coupling between the approximate guided modes  $\phi_1$  and  $\phi_2$ .

## B. Background fields and Green's function

In this section we will derive the necessary expressions for the background field and the associated Green's function. As in the main section we assume that the dielectric function  $\epsilon_0(z)$  approaches 1 for  $z \rightarrow -\infty$ .

### 1. TE waves

We start with Eq.(12) for the Green's function  $g_0(z, z')$  in the TE scattering. Let us denote by  $E_0^{(\pm)}(z)$  two independent solutions of the homogeneous equation (14). Using these solutions the Green's function can be expressed as

$$g_0(z, z') = -\frac{1}{W} \left( \theta(z' - z) E_0^{(+)}(z') E_0^{(-)}(z) + \theta(z - z') E_0^{(+)}(z) E_0^{(-)}(z') \right). \quad (149)$$

where  $W$  is the ( $z$ -independent) Wronskian

$$W = \frac{dE_0^{(+)}(z)}{dz} E_0^{(-)}(z) - E_0^{(+)}(z) \frac{dE_0^{(-)}(z)}{dz}. \quad (150)$$

This is easily verified by observing that by construction the Green's function satisfies Eq.(12) for  $z \neq z'$ . Furthermore the prefactor  $-1/W$  is found by integrating (12) over  $z$  in an infinitesimal interval around  $z'$ .

The choice of the two linearly independent solutions  $E_0^{(\pm)}(z)$  is dictated by the type of the Green function one needs. It is convenient to require that  $g_0(z, z')$  as a function of  $z$  for the values of  $z'$  inside the grating behaves as a reflected (transmitted) wave in the  $z \rightarrow -\infty$  ( $z \rightarrow \infty$ ) region far away from the grating. This leads to the boundary conditions

$$\lim_{z \rightarrow \infty} E_0^{(+)}(z) = t_0^+(\omega) e^{ik_z^+ z}, \quad \lim_{z \rightarrow -\infty} E_0^{(-)}(z) = t_0^-(\omega) e^{-ik_z^- z} \quad (151)$$

with  $k_z^\pm$  denoting the  $z$ -component of the incident wave vector in the two asymptotic regions

$$k_z^+ = \omega \sqrt{\epsilon_{IV} - \sin^2 \theta}, \quad k_z^- = \omega \sqrt{\epsilon_I - \sin^2 \theta}. \quad (152)$$

These equations describe electric fields incident from above ( $E_0^+$ ) or below ( $E_0^-$ ) (cf. Fig. 1). Their normalization is fixed by the amplitude of the incident wave which we choose as

$$\lim_{z \rightarrow -\infty} E_0^{(+)}(z) = e^{ik_z^- z} + r_0^+(\omega) e^{-ik_z^- z}, \quad \lim_{z \rightarrow \infty} E_0^{(-)}(z) = e^{-ik_z^+ z} + r_0^-(\omega) e^{ik_z^+ z}. \quad (153)$$

Evaluating  $W$  in region IV yields

$$W = -2ik_z^+ t_0^+(\omega) \quad (154)$$

Equally well the Wronskian can be calculated in region I yielding the relation

$$|r_0^+(\omega)|^2 + \frac{k_z^+}{k_z^-} |t_0^+(\omega)|^2 = 1. \quad (155)$$

The two solutions  $E_0^{(\pm)}(z)$  are related to each other

$$E_0^{(-)}(z) = \frac{1}{t_0^{+\star}(\omega)} (E_0^{(+)\star}(z) - r_0^{+\star} E_0^{(+)}(z)). \quad (156)$$

The Green's function at large negative  $z$  is needed in the computation of the reflection amplitude

$$\lim_{z \rightarrow -\infty} g_0(z, z') = \frac{1}{2ik_z^-} e^{-ik_z^- z} E_0^{(+)}(z'). \quad (157)$$

We also need the spectral representation of the Greens-function

$$g_0(k_z, z, z') = \frac{1}{2\pi} \int dk'_z \frac{E_0^{(+)}(k'_z, z) E_0^{(+)\star}(k'_z, z')}{k_z^2 - k'^2 + i\epsilon}. \quad (158)$$

Here we have made explicit the dependence of the fields and the Green's function on the incident wave vector. Again it is obvious that for  $z \neq z'$  the Green's function satisfies Eq.(12). With the help of the completeness relation

$$\int dk'_z E_0^{(+)}(k'_z, z) E_0^{(+)\star}(k'_z, z') = 2\pi \delta(z - z'), \quad (159)$$

the correct form of the singularity in Eq.(12) is confirmed. Using the decomposition of the denominator into principal value and  $\delta$  function contributions

$$\frac{1}{k_z^2 - k_z'^2 + i\epsilon} = \frac{P}{k_z^2 - k_z'^2} - i\pi\delta(k_z^2 - k_z'^2),$$

the imaginary part of the Green's function is obtained

$$\text{Im } g_0(k_z, z, z') = -\frac{1}{4k_z^-} \left[ E_0^{(+)}(k_z, z) E_0^{(+)*}(k_z, z') + E_0^{(+)*}(k_z, z) E_0^{(+)}(k_z, z') \right]. \quad (160)$$

## 2. TM waves

The Green's function  $g_0(z, z')$  for the TM case, Eq. (37), is found in the same way as for the TE scattering. We denote two independent solutions of the homogeneous equation (i.e. of Eq. (37) with the right hand side set to zero) by  $H_0^{(\pm)}(z)$ . Then

$$g_0(z, z') = \nu \left[ H_0^{(+)}(z) H_0^{(-)}(z') \theta(z - z') + H_0^{(+)}(z') H_0^{(-)}(z) \theta(z' - z) \right] \quad (161)$$

with a  $z$ -independent constant  $\nu$  which is found by integrating (37) over  $z$  in an infinitesimal interval around  $z'$ . The only subtlety relative to the TE case is the presence of the  $\partial_z \gamma(z) \partial_z$  in the defining equation (37). This leads to two modifications relative to the TE case. On one hand the expression for  $\nu$  is now

$$\nu = -\frac{1}{\gamma_0(z) W(z)}. \quad (162)$$

where  $W(z) = H_0^{(+)} \partial_z H_0^{(-)} - H_0^{(-)} \partial_z H_0^{(+)}$  is the Wronskian of the two solutions. On the other hand the Wronskian of any two solutions like  $H_0^{(\pm)}(z)$  is not a constant but obeys the so called Abel formula written in our case as  $\gamma_0(z) W(z) = \text{constant}$ . Together we have that  $\nu$  is indeed independent of  $z$  and can be calculated in a convenient point.

We again choose the solutions  $H_0^{(+)}(z)$  and  $H_0^{(-)}(z)$  such that  $g_0(z, z')$  behaves as a reflected (transmitted) wave when  $z'$  is finite and  $z \rightarrow -\infty$  ( $z \rightarrow \infty$ ). This leads to the conditions

$$z \rightarrow -\infty : \quad H_0^{(-)}(z) \rightarrow t_0^- e^{-ik_z^- z}; \quad z \rightarrow \infty : \quad H_0^{(+)}(z) \rightarrow t_0^+ e^{ik_z^+ z} \quad (163)$$

with

$$z \rightarrow \infty : \quad H_0^{(-)}(z) \rightarrow e^{-ik_z^+ z} + r_0^+ e^{ik_z^+ z}; \quad z \rightarrow -\infty : \quad H_0^{(+)}(z) \rightarrow e^{ik_z^- z} + r_0^- e^{-ik_z^- z}. \quad (164)$$

At  $z \rightarrow -\infty$  we have  $\gamma(z \rightarrow -\infty) = 1/\epsilon_I$  and  $W(z \rightarrow -\infty) = -2ik_z^- t_0^-$  so that

$$\nu = -\frac{i\epsilon_I}{2k_z^- t_0^-} \quad (165)$$

Using in Eq. (69) the asymptotic expressions for  $H_0^{(\pm)}(z)$  and the Green's function (161) we obtain the result (73).

### C. Dealing with singular expressions in the description of TM resonances

The derivative terms in the operators  $\Theta_{k0}$  and  $\Theta_{0k}$  contain combinations  $\partial_z \epsilon_k(z) \partial_z$  which produce  $\delta$ -function like singularities when acting on  $H_0^\pm(z)$ ,  $\mathcal{H}_{k,\kappa}$  and  $g_0(z, z')$ . Here we will explain how we have regularized such expressions. Let us consider as an example the expression (72) for  $\Sigma$ . Our strategy is to start with narrow but continuous transition layers between the dielectric layers. We then transform this expression in such a way that in the limit of sharp boundaries i.e. zero transition layers width it will not contain ambiguous singularities. Let us demonstrate this for the term of (72) which contains the differential operator parts of both  $\Theta_{k0}$  and  $\Theta_{0k}$

$$\begin{aligned} & \int dz dz' \mathcal{H}_{k,\kappa}(z) \partial_z \gamma_k(z) \partial_z g_0(z, z') \partial_{z'} \gamma_{-k}(z') \partial_{z'} \mathcal{H}_{k,\kappa}(z') = \\ &= \int dz dz' [\partial_z \mathcal{H}_{k,\kappa}(z)] \gamma_k(z) [\partial_z \partial_{z'} g_0(z, z')] \gamma_{-k}(z') [\partial_{z'} \mathcal{H}_{k,\kappa}(z')] \rightarrow \end{aligned} \quad (166)$$

$$\rightarrow |\gamma_k|^2 \int_{I_g} dz dz' [\partial_z \mathcal{H}_{k,\kappa}(z)] [\partial_z \partial_{z'} g_0(z, z')] [\partial_{z'} \mathcal{H}_{k,\kappa}(z')] \quad (167)$$

where we started with infinite integration range assuming that  $\gamma_{\pm k}(z)$  tend to zero fast but continuously outside the grating layer. In integrations by parts the surface terms vanish while the resulting integral has only finite discontinuities in the limit of sharp boundaries. Such discontinuities do not cause ambiguities so that the limit can safely be taken. The other two terms containing differential operators in (72) can be regularized in the same manner.

The above procedure can be conveniently summarized by stating that expressions like (72) should be used with the operators  $\Theta_{nm}$  replaced by

$$\Theta_{nm} \rightarrow \gamma_{n-m} [\overleftarrow{\partial_z} \overrightarrow{\partial_z} + (k_z + nK_g)(k_x + mK_g)] \quad (168)$$

where the arrow above the derivative indicates that it acts on the function to the right or to the left of it depending on the direction of the arrow.

We also note a useful identity

$$\begin{aligned} \partial_z \partial_{z'} g_0(z, z') &= \nu [\partial_z H_0^{(+)}(z) \partial_{z'} H_0^{(-)}(z') \theta(z - z') + \partial_{z'} H_0^{(+)}(z') \partial_z H_0^{(-)}(z) \theta(z' - z)] - \\ &\quad - 1/\gamma_0(z) \delta(z - z') \end{aligned} \quad (169)$$

which is obtained by differentiating Eq. (161) and using (162).

### Acknowledgments

F.L. is grateful for the support and the hospitality at the Department of Condensed Matter, Weizmann Institute. This work is supported in part by the Albert Einstein Minerva Center for Theoretical Physics and by a grant from Israeli Ministry of Science.

- 
- [1] H. Feshbach, *Ann. of Phys.* **5**, 357, (1958)
  - [2] H. Feshbach, *Ann. of Phys.* **19**, 287, (1962)

- [3] H. Feshbach, Theoretical Nuclear Physics, Nuclear Reactions, John Wiley & Sons (1992)
- [4] E. Timmermans, P. Tommasini, M. Hussein, A. Kerman, *Phys. Rep.* **315**, 199, (1999)
- [5] C. Chin, R. Grimm, P. Julienne and E. Tiesinga, *Rev. Mod. Phys.* **82**, 1225, (2010)
- [6] L. Mashev and E. Popov, *Optics Comm.* **55**, 377, (1985)
- [7] G. A. Golubenko, A. S. Svakhin, V. A. Sychugov, and A. V. Tishchenko, *Sov. J. Quantum Electron.* **15**, 886 (1985)
- [8] O. Katz, J. M. Levitt, E. Grinvald, and Y. Silberberg, *Opt. Express* **18**, 22693, (2010)
- [9] S. S. Wang and R. Magnusson, *Appl. Opt.* **32**, 2606, (1993)
- [10] R. Magnusson, M. Shokooh-Saremi, and E. G. Johnson, *Opt. Lett.* **35**, 2472, (2010)
- [11] F. Brückner, D. Friedrich, T. Clausnitzer, M. Britzger, O. Burmeister, K. Danzmann, E. Kley, A. Tünnermann, and R. Schnabel, *Phys. Rev. Lett.* **104**, 163903, (2010)
- [12] D. Fattal, J. Li, Z. Peng, M. Fiorentino, and R. G. Beausoleil, *Nature Photon.* **4**, 466, (2010)
- [13] M. Lu, S. S. Choi, C. J. Wagner, J. G. Eden, and B. T. Cunningham, *Appl. Phys. Lett.* **92**, 261502, (2008)
- [14] A.-L. Fehrembach, D. Maystre, and A. Sentenac, *J. Opt. Soc. Am. A* **19**, 1136, (2002)
- [15] S. Fan, W. Suh, and J. D. Joannopoulos, *Journal of the Optical Society of America A*, **20**, 569, (2003)
- [16] S. Fan, J. D. Joannopoulos, *Phys. Rev. B* **65**, 235112, (2002)
- [17] K. Koshino, *Phys. Rev. B* **67**, 165213, (2003)
- [18] D. Rosenblatt, A. Sharon, and A. A. Friesem, *IEEE J. Quant. Electron.* **33**, 2038, (1997)
- [19] M. G. Moharam, E. B. Grann, D. A. Pommet, T. K. Gaylord, *J. Opt. Soc. Am. A* **12**, 1077, (1995)
- [20] P. Sheng, R. S. Stepleman and P. N. Sanda, *Phys. Rev. B* **26**, 2907, (1982)
- [21] R. Kazarinov and C. Henry, *IEEE J. Quant. Electron.* **21**, 144, (1985)
- [22] A. E. Miroshnichenko, *Phys. Rev. E* **79**, 026611, (2009)
- [23] A. E. Miroshnichenko, S. Flach, and Y. S. Kivshar, *Rev. Mod. Phys.* **82**, 2257, (2010)
- [24] Ming Kang, Hai-Xu Cui, Yongnan Li, Bing Gu, Jing Chen and Hui-Tian Wang *J. Appl. Phys.* **109**, 014901 (2011)
- [25] A. Donval, J. Toussaere, E. Zyss, G. Levy-Yurista, E. Jonsson, and A. A. Friesem, *Synthetic Metals* **124**, 19, (2001)
- [26] O. Boyko, F. Lemarchand, A. Talneau, A.-L. Fehrembach, and A. Sentenac, *J. Opt. Soc. Am. A* **26**, 676, (2009)
- [27] Z. S. Liu, S. Tibuleac, D. Shin, P. P. Young, and R. Magnusson, *Opt. Lett.* **23**, 1556, (1998)
- [28] T. Katchalski, G. Levy-Yurista, A. A. Friesem, G. Martin, R. Hierle, and J. Zyss, *Opt. Express* **13**, 4645, (2005)
- [29] J. D. Joannopoulos, S. G. Johnson, J. W. Winn and R. D. Meade, *Photonic Crystals Molding the Flow of Light*, Princeton University Press, (2008)
- [30] U. Fano, *Nuovo Cimento*, **12**, 156, (1935)
- [31] U. Fano, *Phys. Rev.* **124** 1866, (1961)
- [32] P. Markoš, C. M. Soukoulis, *Wave Propagation*, Princeton University Press, (2008)
- [33] L. Li, *J. Opt. Soc. Am. A* **13**, 1870, (1996)
- [34] G. Granet and B. Guizal, *J. Opt. Soc. Am. A* **13** 1019, (1996)
- [35] P. Lalanne, and G. M. Morris, *J. Opt. Soc. Am. A* **13** 779, (1996)
- [36] E. Popov, and M. Nevier, *J. Opt. Soc. Am. A* **17** 1773, (2000)
- [37] N. M. Lyndin, O. Parriaux and A. V. Tishenko, *J. Opt. Soc. Am. A* **24**, 3781, (2007)
- [38] W. L. Barnes, T. W. Preist, S. C. Kitson, and J. R. Sambles, *Phys. Rev. B*, **54**, 6227, (1996)

- [39] N. Bloembergen, E. M. Purcell, and R. V. Pound em *Phys. Rev.* **73**, 679, (1948)
- [40] R. H. Dicke, *Phys. Rev.* **93**, 99, (1954)
- [41] D. Pavolini, A. Crubellier, P. Pillet, L. Cabaret, and S. Liberman, *Phys. Rev. Lett.* **54**, 1917, (1985)
- [42] S. E. Harris, *Physics Today* **50**, 36, (1997)
- [43] C. L. G. Alzar, M. A. G. Martinez, and P. Nussenzweig, *American Journal of Physics* **70**, 37, (2002)
- [44] M. F. Yanik, W. Suh, Z. Wang, and S. Fan, *Phys. Rev. Lett.* **93**, 233903, (2004)
- [45] C. Mahaux and H. A. Weidenmüller, *Shell-Model Approach to Nuclear Reactions*, North-Holland Publishing Company (1969)
- [46] P. von Brentano, *Phys. Lett. B* **238**, 1, (1990)
- [47] B. M. Nestmann, 1998 *J. Phys. B: At. Mol. Opt. Phys.* **31** 3929, (1998)